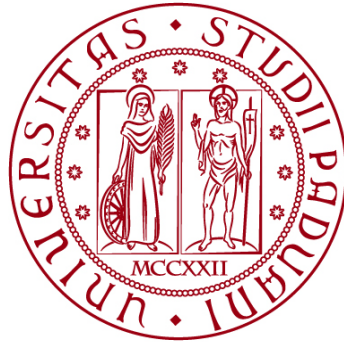


**UNIVERSITÀ DEGLI STUDI DI PADOVA**

**DIPARTIMENTO DI BIOLOGIA**

**Corso di Laurea in Biologia Molecolare**



**ELABORATO DI LAUREA**

**L'assenza di Parkin non promuove la  
disfunzione di dopamina o del mitocondrio  
in topi mutatori mitocondriali *PolgA*<sup>D257A/D257A</sup>**

**Tutor: Prof.ssa Natascia Tiso  
Dipartimento di Biologia**

**Co-tutor: Dott.ssa Raquel Brañas Casas  
Dipartimento di Biologia**

**Laureando: Zhangyu Zhu**

**ANNO ACCADEMICO 2023/2024**

## Abstract

La malattia di Parkinson è una malattia neurodegenerativa incurabile caratterizzata da deficit motori progressivi tra i quali tremore, rigidità, instabilità posturale e bradicinesia. Durante gli stadi successivi della malattia possono comparire ulteriori sintomi non motori, quali disfunzione autonoma, dolore e declino cognitivo. La malattia di Parkinson è la seconda patologia neurodegenerativa più comune, la cui prevalenza aumenta con l'età; il numero di decessi e di anni di vita corretti per disabilità sono tra i più elevati tra le malattie neurologiche. PARK2 è il gene mutato più comune nei casi familiari monogenici recessivi della malattia di Parkinson. Le mutazioni patogene causano una perdita di funzione della proteina codificata, l'ubiquitina E3 ligasi "Parkin". I substrati dell'ubiquitinazione di Parkin interessano sostanzialmente l'intera dinamica mitocondriale. In vari modelli animali, attraverso la mutazione del gene Polg, sono stati prodotti individui con invecchiamento prematuro e delezioni cumulative del DNA mitocondriale (mtDNA). Lo studio in oggetto ha mirato a combinare le mutazioni di Parkin e Polg per analizzarne simultaneamente il ruolo nella malattia di Parkinson. L'animale modello selezionato è il topo, data la sua anatomia e fisiologia simile a quella umana. Lo studio dimostra che i topi doppi mutanti per Parkin e Polg non mostrano neuro-degenerazione dopaminergica né deficit motori dipendenti dal sistema nigro-striatale. Inoltre, la perdita di Parkin non sinergizza con la disfunzione mitocondriale indotta da Polg. In sostanza, lo studio evidenzia che i topi doppi mutanti per Parkin e Polg non rappresentano un modello completamente fedele per la malattia di Parkinson.

## Indice

1. Stato dell'arte: la malattia di Parkinson	3
1.1 Epidemiologia	3
1.2 Genetica e patofisiologia	3
1.2.1 Disfunzione mitocondriale nel Parkinsonismo	3
1.2.2 Gene <i>PRKN</i> e controllo di qualità mitocondriale	4
1.3 <i>POLG</i>	6
1.4 Parkinsonismo e <i>POLG</i>	7
2. Approccio sperimentale: materiali, metodi e risultati	7
2.1 Immunoistochimica e conta stereologica dei neuroni	8
2.2 Tecnica di HPLC	8
2.3 Western blot e attività degli enzimi mitocondriali	12
2.4 Real-time quantitative PCR	14
3. Discussione dei risultati	15
3.1 Difficoltà a modellizzare il Parkinsonismo in topo	15
3.2 Risultati del Western blot	16
3.3 Test di deficit non motori	17
3.4 Risultati della Quantitative PCR	18
3.4.1 Numero di copie di mtDNA e delezione del mtDNA	18
3.4.2 La diminuzione di <i>COXI</i>	19
3.4.3 L'aumento del <i>D-loop</i>	20
4. Conclusioni	20
5. Bibliografia	21
6. Appendice	22

## 1. Stato dell'arte: la malattia di Parkinson

### 1.1 Epidemiologia

La malattia di Parkinson (Parkinson's disease o PD) è la seconda malattia neurodegenerativa più comune tra tutte le malattie neurologiche e quella in più rapida crescita in termini di decessi, anni di vita corretti per disabilità e prevalenza; non esiste una cura per tale malattia. Il Parkinsonismo è una complessa malattia neurodegenerativa progressiva caratterizzata da deficit motori progressivi tra cui tremore, rigidità, instabilità posturale e bradicinesia. Durante gli stadi successivi della malattia possono comparire ulteriori sintomi non motori, quali disfunzione autonoma, dolore e declino cognitivo. Tuttavia, ci sono molti sintomi non motori associati al Parkinsonismo che possono comparire anni, a volte decenni, prima dell'esordio di un fenotipo neuromotorio distinto. Questi sintomi includono iposmia, anomalie del sonno, disturbi gastrointestinali, ansia, depressione, disfunzione autonoma e disturbi cognitivi. Le cause di PD sono complesse e la maggior parte hanno un'eziologia multifattoriale, ossia sono il risultato di una combinazione di fattori ambientali e fattori genetici [1]. L'esposizione a sostanze chimiche tossiche e lesioni alla testa aumentano il rischio di PD; la prevalenza del Parkinsonismo aumenta con l'età. I sintomi motori di PD sono causati dalla morte dei neuroni che producono dopamina (DA) all'interno della substantia nigra pars compacta (SNpc), con conseguente deplezione di DA nello striato. La deplezione della DA striatale è accompagnata dalla comparsa dei corpi di Lewy (LB), caratteristiche inclusioni intra-citoplasmatiche all'interno dei neuroni sopravvissuti.

### 1.2 Genetica e patofisiologia

Storicamente, il Parkinsonismo era considerata una malattia sporadica in cui i fattori ambientali e l'età rappresentavano i principali fattori di rischio fino all'identificazione negli anni '90 del gene SNCA, codificante la proteina  $\alpha$ -sinucleina ( $\alpha$ -Syn), come gene causale. Successivamente sono stati identificati ben 90 geni potenzialmente associati al PD. La maggior parte di questi geni ospitano mutazioni rare non funzionalmente convalidate e pertanto ancora presunte. Di questi, solo i geni SNCA, GBA, LRRK2, VPS35, PRKN, PINK1 e PARK7 sono in grado di causare PD monogenico, con vari gradi di penetranza, e sono stati associati in modo convincente al tipico PD. Sebbene i pazienti con PD monogenico rappresentino il 10-20% dei casi, gli studi dei geni monogenici di Parkinsonismo e la caratterizzazione dei loro prodotti proteici hanno portato a conoscenze cruciali sui meccanismi di PD sia sporadico che familiare. Inoltre, fattori di stress ambientale o altri fattori esterni possono attivare o inibire le proteine implicate nel PD monogenico familiare, collegandole così al PD sporadico [2].

#### 1.2.1 Disfunzione mitocondriale nel Parkinsonismo

Alla fine degli anni '70 l'esposizione accidentale alla 1-metil-4-fenil-1,2,3,6-tetraidropiridina (MPTP) [3], ha collegato la disfunzione mitocondriale al morbo di

Parkinson. L'MPTP inibisce il complesso I, un componente del meccanismo della fosforilazione ossidativa della catena respiratoria mitocondriale, portando al Parkinsonismo [3].

In effetti, le proteine mutanti prodotte nel PD monogenico partecipano in vie cellulari unificanti, conducendo in misura maggiore o minore ad un deficit del controllo di qualità mitocondriale e alla disfunzione mitocondriale. La perdita della funzione di GCase1 (codificata dal gene *GBA*) e  $\alpha$ -Syn (codificata dal gene *SNCA*) concorrono ad un circuito di feedback positivo patologico che promuove l'aggregazione di  $\alpha$ -Syn. Le varianti  $\alpha$ -Syn formano aggregati resistenti alla degradazione; l'aggregazione di  $\alpha$ -Syn induce indirettamente l'inattivazione di Parkin (codificata da gene *PARK2*) e porta all'accumulo di substrati di Parkin. Le mutazioni di LRRK2 (codificata dal gene *LRRK2*) portano all'inattivazione di PINK1/Parkin. VPS35 (codificata dal gene *VPS35*) e PINK1/Parkin mediano la formazione delle vescicole derivate dai mitocondri (MDV) e partecipano alla regolazione delle dinamiche di fissione/fusione. DJ-1 (codificata dal gene *PARK7*) protegge i mitocondri dal danno ossidativo. Esiste un'interazione genetica bidirezionale tra Parkin/PINK1 e DJ-1, suggerendo che potrebbero agire insieme o in parallelo per preservare la funzione mitocondriale. Parkin e PINK1 (codificata dal gene *PINK1*) sono due proteine strettamente interagenti che funzionando insieme come rilevatore di danno mitocondriale e cooperano nelle vie di controllo della qualità mitocondriale [2].

#### 1.2.2 gene *PRKN* e controllo di qualità mitocondriale

Le mutazioni nei geni *PRKN* e *PINK1* sono rispettivamente prima e seconda causa più comune di PD autosomico recessivo. Le varianti del gene *PRKN* e del gene *PINK1* comprendono in entrambi i casi mutazioni con perdita di funzione. Le proteine codificate da questi due geni si concentrano sull'indirizzamento dei mitocondri aberranti verso la via della mitofagia [2].

Il gene *PINK1* codifica una serina/treonina chinasi da 581 aminoacidi (PINK1). In assenza degli stress mitocondriali, PINK1 penetra la membrana mitocondriale esterna (OMM) e viene scissa, dalle proteasi legate alla membrana mitocondriale interna (IMM), in frammenti che vengono rilasciati nel citosol e degradati tramite ubiquitinazione. Gli stress mitocondriali come la depolarizzazione della membrana, la disfunzione del complesso della catena di trasporto degli elettroni (ETC), lo stress mutageno e lo stress proteotossico compromettono il trasporto attraverso l'OMM, prevenendo così la proteolisi di PINK1. Ciò si traduce nell'accumulo di PINK1 sull'OMM, portando alla dimerizzazione e all'attivazione del dominio chinasi.

Il gene *PRKN* codifica la proteina Parkin, un'ubiquitina ligasi E3 composta da 465 aminoacidi che coniuga catene di mono o poli-ubiquitina alle proteine substrato. L'ubiquitinazione è un'importante modifica post-traduzionale che si basa sulle azioni sequenziali degli enzimi che attivano l'ubiquitina, degli enzimi coniuganti

(E2) e delle ligasi (E3) per controllare la funzione e il destino delle proteine. Parkin è una proteina autoinibita; esistono interazioni interdominio con regolazione negativa, all'interno della proteina, che devono essere superate durante l'attivazione di Parkin. L'attività chinasi di PINK1 è necessaria per il reclutamento e l'attivazione di Parkin sui mitocondri aberranti.

Una volta reclutata e attivata nei mitocondri, Parkin catalizza la formazione di catene di ubiquitina su varie proteine dell'OMM; queste catene di ubiquitina funzionano come substrati per la fosforilazione di PINK1, reclutando quindi più molecole di Parkin. Il processo dell'eliminazione dei mitocondri aberranti è detto mitofagia; è un processo del controllo di qualità mitocondriale [2]. Il controllo di qualità mitocondriale è un termine onnicomprensivo che include il mantenimento della funzione mitocondriale, il turnover mitocondriale tramite mitofagia e la generazione di nuovi mitocondri. I meccanismi di controllo della qualità mitocondriale possono essere ampiamente classificati in meccanismi di fissione e fusione, degradazione dei mitocondri danneggiati tramite la mitofagia e meccanismi che mediano la biogenesi.

PINK1/Parkin potrebbero avere ruoli opposti nell'indurre la fusione e la fissione mitocondriale in diversi tipi di cellule; in alternativa, potrebbero svolgere un ruolo nel mantenimento dell'equilibrio tra questi due processi e la loro perdita o inattivazione potrebbe promuovere l'uno o l'altro processo a seconda dell'ambiente locale o del tipo di cellula. La fusione mitocondriale è controllata da tre principali proteine GTPasi: mitofusina1 (Mfn1), mitofusina2 (Mfn2) e atrofia ottica 1 (OPA1); la fissione è regolata da Drp1. Parkin è necessaria per l'oligomerizzazione di Mfn 1 e l'attivazione di Drp1; la fissione e la formazione dell'autofagosoma sono accoppiate nella mitofagia. Parkin/PINK1 mediano anche la generazione di MDV; la via è indipendente da Drp1 e rappresenta un meccanismo selettivo che rimuove i componenti mitocondriali danneggiati senza compromettere la funzione mitocondriale complessiva.

La rimozione dei mitocondri danneggiati deve essere seguita dalla sintesi di nuovi mitocondri; Parkin/PINK1 promuovono la biogenesi mitocondriale attraverso la degradazione di PARIS (ZNF746). PARIS è una proteina in grado di reprimere la trascrizione di PGC-1 $\alpha$ . PGC-1 $\alpha$  è un regolatore fondamentale della biogenesi mitocondriale; la sovra-espressione di PGC-1 $\alpha$  ripristina la biogenesi mitocondriale, aumenta il numero e la funzione mitocondriale, mentre la perdita dell'espressione di PGC-1 $\alpha$  riduce significativamente l'espressione delle trascrizioni mitocondriali e la funzione mitocondriale. PINK1 fosforila PARIS, preparandola all'ubiquitinazione mediante degradazione di Parkin e del proteasoma. PARIS si accumula a causa della perdita o dell'inattivazione di Parkin, portando alla sotto-regolazione di PGC-1 $\alpha$ , alla compromissione della biogenesi mitocondriale e alla degenerazione dei neuroni DA nella SNpc [4].

### 1.3 *POLG*

I mitocondri ospitano le catene di trasporto degli elettroni (ETC) e generano oltre il 90% dell'ATP cellulare attraverso la fosforilazione ossidativa. Le cellule contengono una rete interconnessa di centinaia o talvolta migliaia di mitocondri [6]. In ciascuno mitocondrio si trovano copie multiple del genoma mitocondriale (mtDNA). Ogni copia si presenta come una molecola circolare compatta nella matrice mitocondriale. Il mtDNA è suscettibile a danni, quali tossine ambientali, radiazioni, ossidazione ed errori di replicazione intrinseci. L'assenza di efficaci vie di riparazione del DNA nelle cellule di mammifero espone il mtDNA a un rischio maggiore di accumulo di lesioni non riparate, che possono portare alla fissazione di mutazioni, grandi delezioni e blocchi della replicazione e della trascrizione. Tuttavia, la replicazione del mtDNA è disaccoppiata dal ciclo cellulare, pertanto è possibile sintetizzare ulteriori copie del mtDNA per alleviare l'impatto del danno sui singoli genomi. Sono stati identificati quattro principali geni nucleari che sono strettamente associati alla replicazione del DNA mitocondriale: *POLG*, *POLG2*, *SSBP1* e *TWNK*. Varianti patologiche delle proteine di replicazione raramente determinano gravi interruzioni della funzione, tuttavia, comportano funzioni biochimiche alterate che spesso determinano sottili cambiamenti nell'attività enzimatica, nell'affinità al DNA o nella stabilità delle proteine o dei complessi. Infine, possono portare ad un aumento dei tassi di errore durante la sintesi del DNA, al disaccoppiamento della forcella di replicazione, all'esposizione di DNA a singolo filamento vulnerabile e ad inefficienze nella replicazione. A sua volta, lo stress replicativo causato da proteine di replicazione disfunzionali porta alla deplezione, delezione e mutazione puntiforme del mtDNA; questo circuito di feedback positivo dell'alterazione, in conseguenza di una grave deplezione o accumulo di danni nel mtDNA, può portare a perturbazioni dell'ETC, interrompere l'omeostasi mitocondriale, ridurre il potenziale di membrana e portare a disfunzione mitocondriale.

Le mutazioni *POLG* possono essere suddivise in mutazioni con ereditarietà autosomica recessiva e con ereditarietà autosomica dominante. I disturbi legati a *POLG* ad esordio precoce e giovanile/adulto sono tipicamente causati da varianti patologiche bi-alleleliche ed ereditati con modalità autosomica recessiva, mentre l'esordio tardivo può essere causato da varianti *POLG* patologiche eterozigoti ed ereditato con modalità autosomica dominante.

Il parkinsonismo è il disturbo del movimento extrapiramidale osservato più frequentemente nei pazienti con mutazioni *POLG*. Le conseguenze delle mutazioni *POLG* possono essere suddivise in due grandi gruppi: delezioni multiple del mtDNA e deplezione del mtDNA. Non sono evidenti correlazioni dirette genotipo-fenotipo per le mutazioni *POLG*: le stesse mutazioni spesso determinano la delezione del mtDNA, la deplezione del mtDNA o entrambe.

## 1.4 Parkinsonismo e *POLG*

La malattia di Parkinson è principalmente una malattia neurodegenerativa cronica e progressiva; pertanto, un modello animale ideale a livello genetico richiederebbe l'accumulo di mutazioni legato all'età. Rispetto alle neurotossine convenzionali, le delezioni o le mutazioni nel gene *POLG* generano stress replicativo e accelerano l'accumulo delle mutazioni nel mtDNA con conseguente danno mitocondriale, dunque soddisfano i requisiti della progressività e della dipendenza dall'età nel simulare il Parkinsonismo. Introducendo mutazioni *POLG* autosomiche recessive (*PolgA<sup>D257A/D257A</sup>*), si è riusciti a generare una linea di topi sperimentali che mostravano caratteristiche quali il progressivo accumulo di mutazioni del DNA mitocondriale e la concomitante compromissione della funzione di fosforilazione ossidativa (OXPHOS).

Le cellule del sistema nervoso centrale presentano sfide energetiche uniche a causa della loro polarizzazione strutturale, delle richieste energetiche e della longevità. Esse sono particolarmente suscettibili al danno mitocondriale e al deterioramento funzionale che probabilmente inizia con la delezione e deplezione del DNA mitocondriale; pertanto, si affidano maggiormente al controllo di qualità mitocondriale per eliminare i mtDNA aberranti. Teoricamente, una chimera tra *PolgA<sup>D257A/D257A</sup>* e deplezione di *PRKN* dovuta all'effetto sinergico tra *Polg* e *PRKN*, con *PolgA<sup>D257A/D257A</sup>* che contribuisce all'aumento delle delezioni (e/o deplezione) del mtDNA e contemporaneamente con *Parkin<sup>-/-</sup>* che porta alla disfunzione dei meccanismi di riparazione del mtDNA e quindi alla disfunzione mitocondriale, potrebbe simulare il Parkinsonismo in modelli murini. Tuttavia, nella realtà non è sperimentalmente semplice raggiungere questo obiettivo.

## 2. Approccio sperimentale: materiali, metodi e risultati

In questo studio, è stato generato un modello transgenico *Parkin<sup>-/-</sup>/PolgA<sup>D257A/D257A</sup>* incrociando topi *Parkin<sup>-/-</sup>* con topi *PolgA<sup>D257A/D257A</sup>*. Sono stati confrontati i quattro genotipi di topi utilizzati nell'esperimento: WT (*Parkin<sup>+/+</sup>/PolgA<sup>+/+</sup>*), *Parkin<sup>-/-</sup>*, *PolgA<sup>D257A/D257A</sup>* e *Parkin<sup>-/-</sup>/PolgA<sup>D257A/D257A</sup>*. Si è studiato se esistesse un sinergismo sulla disfunzione mitocondriale conseguente alla perdita di Parkin nei modelli murini di deficit mitocondriali. Si è analizzato se il modello transgenico potesse simulare la perdita progressiva di neuroni dopaminergici nella substantia nigra pars compacta, caratteristica del Parkinsonismo, e la disfunzione motoria neuro-comportamentale specifica nigro-striatale.

L'attenzione è stata focalizzata sui risultati delle tecniche e sulle analisi molecolari effettuate negli esperimenti: conta stereologica dei neuroni, cromatografia liquida ad alta prestazione (HPLC), Western blot e PCR quantitativa.



## 2.1 Immunoistochimica e conta stereologica dei neuroni

I tessuti encefalici contenenti il mesencefalo ventrale di topo sono stati congelati e poi tagliati in sezioni coronali seriali; le sezioni sono state bloccate e poi incubate con anticorpo primario specifico per la tirosina idrossilasi (TH). Prima del conteggio stereologico le sezioni sono state contro-colorate con Nissl; i neuroni dopaminergici e i neuroni nella substantia nigra del mesencefalo ventrale sono distinguibili con frazionatore ottico (TH positivi e Nissl positivi) e numerabili con il software Stereo investigator.

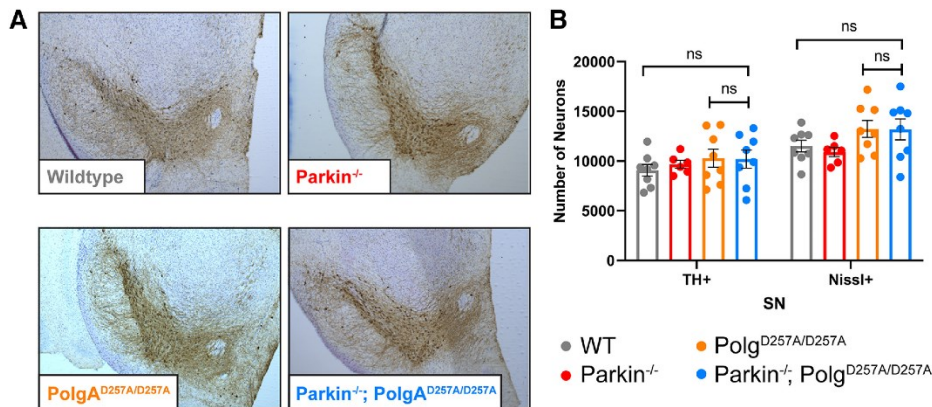


Figura 1 Analisi neuropatologica di tessuto mesencefalico ventrale di topi di 12 mesi. I neuroni TH<sup>+</sup> sono colorati in marrone e i Nissl<sup>+</sup> sono colorati in blu nell'analisi immunoistochimica di sezioni (A). Quantificazione stereologica dei neuroni TH<sup>+</sup> e Nissl<sup>+</sup> nella substantia nigra (B).

La Figura 1A riporta un confronto immediato tra le immagini al microscopio, con un'apparente mancanza di perdita di popolazioni neuronali dopaminergiche nel tessuto del mesencefalo ventrale tra diversi genotipi. Nella Figura 1B la quantificazione di neuroni TH<sup>+</sup> e Nissl<sup>+</sup> tra le coorti mostra come non esista nessun cambiamento evidente nel numero di neuroni dopaminergici tra le quattro coorti.

## 2.2 Tecnica di HPLC

Le concentrazioni di dopamina (DA) e i prodotti relativi di degradazione sono stati determinati mediante HPLC con rilevamento elettrochimico. Inoltre, sono stati calcolati i tassi di turnover della dopamina per valutare la disregolazione delle catecolamine. I prodotti relativi di degradazione della dopamina includono: Acido diidrossifenilacetico (DOPAC), 3-Metossitiramina (3MT), Acido omovanillico (HVA). Inoltre, sono stati determinati la concentrazione di 5-Idrossitriptamina (5HT) e Acido 5-idrossiindolacetico (5HIAA), per valutare il livello di serotonina (un altro neurotrasmettitore regola i neuroni serotonergici), e il turnover di serotonina. La Norepinefrina e l'Epinefrina sono altri neurotrasmettitori della famiglia delle catecolamine; la loro sovra-regolazione sembra un meccanismo compensatorio potenziale in risposta alla perdita di dopamina.

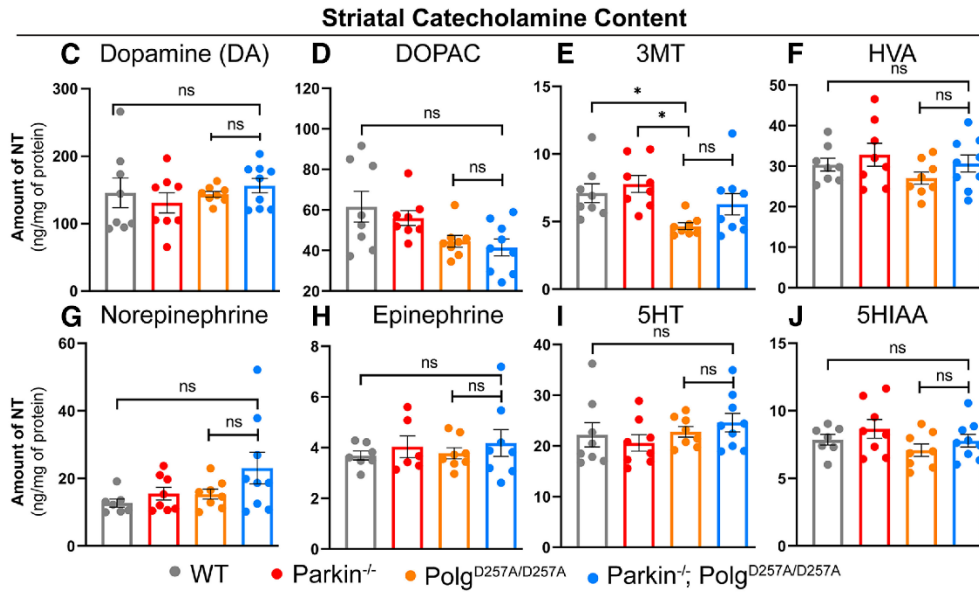


Figura 2 Analisi neuropatologica di tessuto mesencefalico ventrale di topi di 12 mesi. Analisi HPLC del contenuto di dopamina, DOPAC, 3MT, HVA, Norepinefrina, Epinefrina, 5HT e 5HIAA striatale normalizzati rispetto alla concentrazione proteica totale (C-J).

Il contenuto striatale di DA e dei prodotti relativi di degradazione DOPAC, HVA, norepinefrina o epinefrina, come mostrano le immagini dell'analisi neuropatologica (Figura 2C, D, F, G, H), non ha mostrato cambiamenti significativi tra le coorti. E' stata riscontrata una riduzione della 3MT nei topi *PolgA*<sup>D257A/D257A</sup> rispetto sia ai topi wild-type che a quelli *Parkin*<sup>-/-</sup>; tuttavia, non vi era alcuna riduzione nei topi *Parkin*<sup>-/-</sup>/*PolgA*<sup>D257A/D257A</sup> (Figura 2E). Inoltre, il contenuto striatale di 5HT e di 5HIAA non mostrano cambiamenti significativi tra le coorti (Figura 2 I, J).

I tassi di turnover dei due diversi percorsi metabolici della dopamina sono stati calcolati tramite la concentrazione di dopamina e dei suoi prodotti di degradazione: (1) il turnover della dopamina DOPAC-dipendente; (2) il turnover della dopamina 3MT-dipendente.

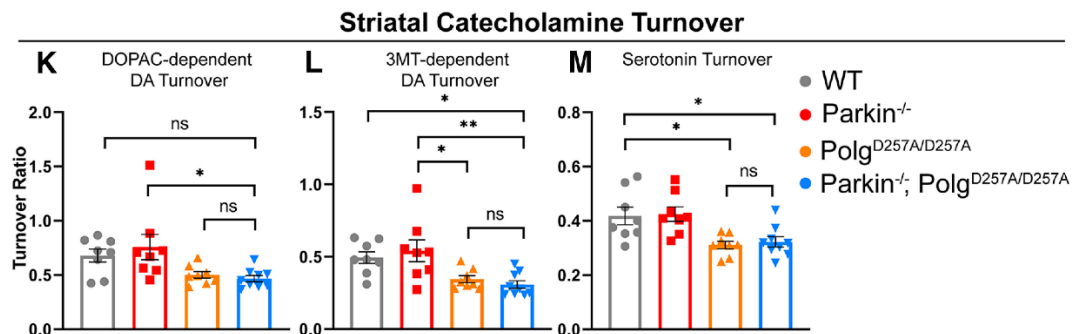


Figura 3 Analisi neuropatologica di tessuto mesencefalico ventrale di topi di 12 mesi. I tassi di turnover della dopamina striatale dipendente da DOPAC valutato da (DOPAC+HVA)/DA (K), i tassi di turnover della dopamina striatale dipendente da 3MT valutato da (3MT+HVA)/DA (L), i tassi di turnover della serotonina striatale valutato mediante 5HIAA/5HT (M).

Utilizzando questo approccio, la Figura 3 K e L riporta le riduzioni sostanziali in entrambi i tipi di percorsi di turnover di DA striatale dei topi *Parkin*<sup>-/-</sup>/*PolgA*<sup>D257A/D257A</sup> rispetto ai topi *Parkin*<sup>-/-</sup>.

Rispetto al topo selvatico, il turnover della dopamina 3MT-dipendente si mostra ridotto statisticamente soltanto nei topi *Parkin*<sup>-/-</sup>/*PolgA*<sup>D257A/D257A</sup> mentre non ha mostrato differenze tra i topi *PolgA*<sup>D257A/D257A</sup> e i topi *Parkin*<sup>-/-</sup>/*PolgA*<sup>D257A/D257A</sup>. Questi risultati implicano che sia i topi *PolgA*<sup>D257A/D257A</sup> che i topi *Parkin*<sup>-/-</sup>/*PolgA*<sup>D257A/D257A</sup> mostrano una certa disregolazione della dopamina striatale senza perdita neuronale dopaminergica; tuttavia la disregolazione è il risultato del knock-in di *PolgA*<sup>D257A/D257A</sup> e non è significativamente influenzata dalla perdita di *Parkin*.

E' stato calcolato il turnover della serotonina tramite la concentrazione di serotonina e del prodotto di degradazione 5HIAA, osservando una riduzione significativa nei topi con deficit di *PolgA* rispetto sia ai topi wild-type che a quelli *Parkin*<sup>-/-</sup> (Figura 3M). Ciò omplica che i topi con deficit di *PolgA* anziani sperimentano una disregolazione delle catecolamine striatali; tuttavia la disregolazione non è rafforzata dalla perdita di *Parkin*.

E' stata misurata la concentrazione di DA, dei prodotti relativi di degradazione di DA, di serotonina, 5HIAA, norepinefrina e epinefrina nel bulbo olfattivo con lo stesso metodo, calcolando il tasso di turnover di dopamina e serotonina nel bulbo olfattivo.

### Olfactory Bulb Catecholamine Content

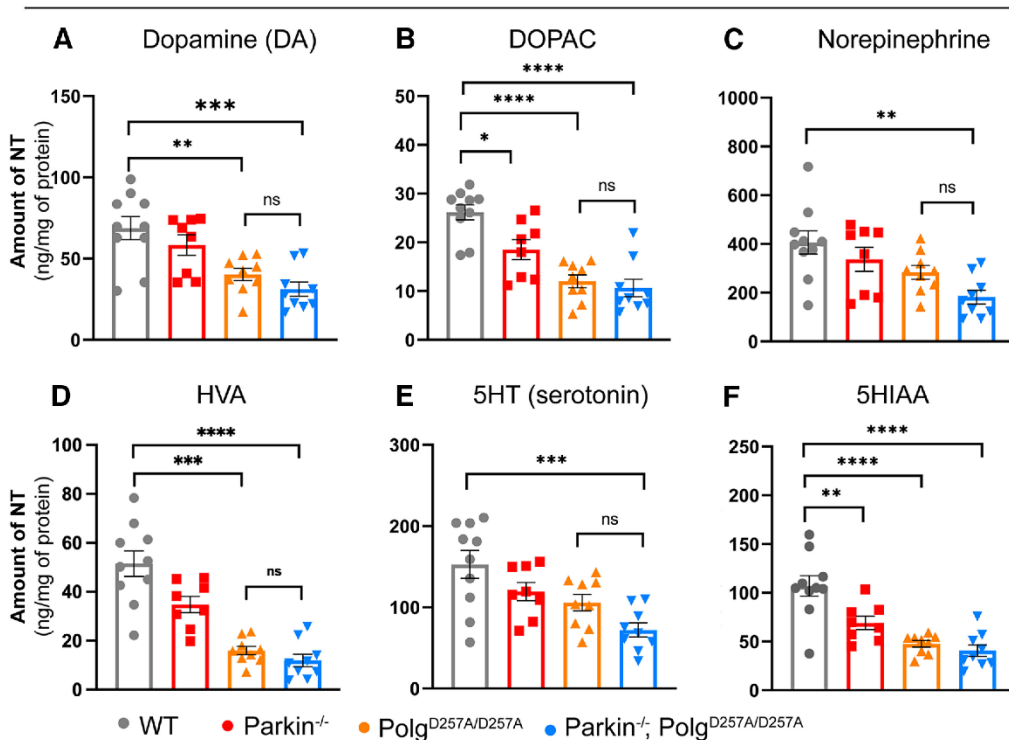
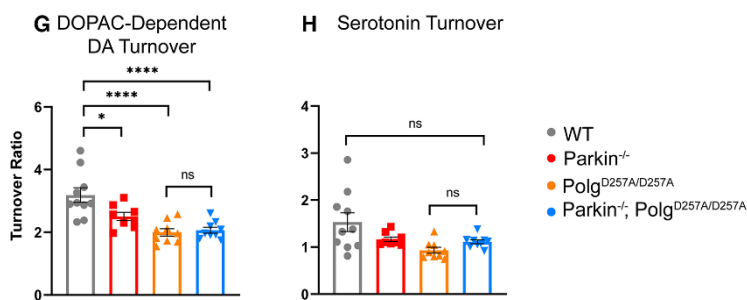


Figura 4 Analisi neuropatologica di tessuto mesencefalico ventrale di topi di 12 mesi. Analisi HPLC del contenuto di dopamina, DOPAC, norepinefrina, HVA, 5HT e 5HIAA nel bulbo olfattivo, normalizzato alla concentrazione proteica totale (A-F).

Le immagini A-F nella Figura 4 riportano una diminuzione significativa della concentrazione di DA, serotonina e prodotti relativi della degradazione nel bulbo olfattivo dei topi con deficit di *PolgA*; tuttavia, queste riduzioni sono indipendenti dalla perdita di *Parkin*. Ulteriori analisi sulla disregolazione delle catecolamine e dell'indolamina sono state effettuate nel bulbo olfattivo.

### Olfactory Bulb Catecholamine Turnover



(G), turnover di 5HT valutato mediante 5HIAA/5HT (H).

Figura 5 Analisi neuropatologica di tessuto mesencefalico ventrale di topi di 12 mesi. Turnover nel bulbo olfattivo della dopamina dipendente da DOPAC valutato da (DOPAC+HVA)/dopamina

Il bulbo olfattivo presenta una diminuzione del turnover della dopamina DOPAC-dipendente nei due tipi di topi con *PolgA*<sup>D257A/D257A</sup>, come mostrato nella Figura 5G, mentre è indipendente dalla perdita di *Parkin*. Sebbene il livello di serotonina e 5HIAA nel bulbo olfattivo presenti una diminuzione netta nei topi con *PolgA*<sup>D257A/D257A</sup> (Figura 4E e F), tuttavia, il turnover di serotonina nel bulbo olfattivo non mostra differenza statisticamente significativa tra le quattro coorti (Figura 5H).

Nello striato, la disregolazione delle catecolamine e dell'indolamina è dovuta alla diminuzione del loro turnover. Nel bulbo olfattivo si riscontra la disregolazione delle catecolamine e la diminuzione del livello della dopamina, tuttavia la disregolazione dell'indolamina appare dovuta alla sola diminuzione del livello di serotonina ed è indipendente dal suo turnover.

### 2.3 Western blot e attività degli enzimi mitocondriali

Le mutazioni del DNA mitocondriale o nucleare portano alla disfunzione primaria della catena respiratoria e conseguenti difetti mitocondriali [7]. Parkin è un attore chiave nella mitofagia, perciò per valutare l'attività del mitocondrio e la mitofagia sono stati monitorati i livelli di espressione delle diverse subunità dei complessi della catena respiratoria e dei marcatori mitofagici. La concentrazione delle proteine da estratto di cervello è stata misurata tramite test BCA (Pierce) e analizzata tramite Western blot. Le proteine sono state trasferite su membrane di PVDF attivate con metanolo. Le proteine trasferite su membrana sono state identificate da anticorpi primari corrispondenti. Successivamente, i Western blot sono stati quantificati tramite Image J. Sono state valutate le seguenti proteine: NDUFA9 (subunità del Complesso I della catena respiratoria), SDHA (complesso II), UQCRC2 (complesso III), COXIV (detto COX4I1) (complesso IV), PDHA (subunità  $\alpha$  1 della piruvato deidrogenasi E1), VDAC (canale 1 anione-selettivo dipendente dalla tensione), LC3I/II (proteine necessarie per la mitofagia), Parkin e  $\beta$ -actina-HRP. Inoltre, è stata misurata l'attività degli enzimi mitocondriali dei complessi I e IV nel tessuto mesencefalico ventrale con i kit ab109721 e ab109911 (Abcam).

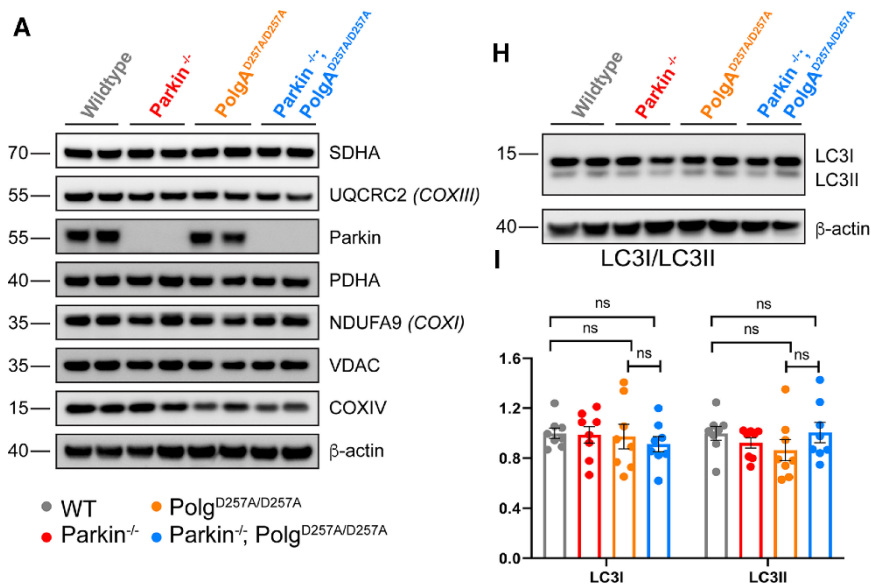


Figura 6 Espressione stazionaria di marcatori mitocondriali e mitofagici nel tessuto mesencefalico ventrale di topi di 12 mesi. Western blot dell'espressione di marcatori mitocondriali (A), Western blot dell'espressione di marcatori mitofagici (H), quantificazione dell'analisi di espressione dei marcatori mitofagici da Western blot (I).

La Figura 6A mostra che la delezione del gene Parkin ha effettivamente provocato l'incapacità di esprimere la proteina Parkin. La Figura 6H e I mostra che i livelli di espressione dei marcatori mitofagici LC3I e LC3II sono mantenuti a livelli stazionari;

non sono state osservate differenze significative tra le coorti, suggerendo che tutti i topi non presentano difetti sostanziali nella mitofagia.

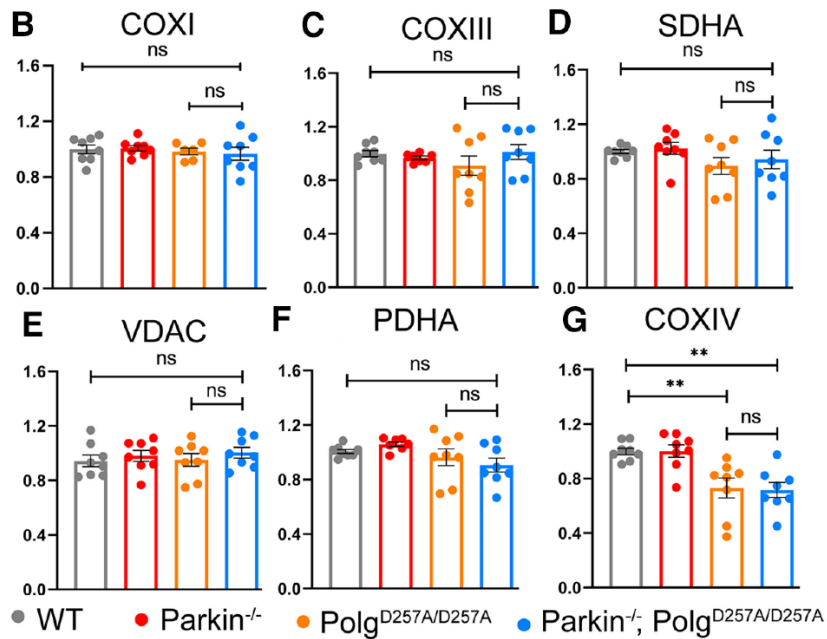


Figura 7 Espressione stazionaria di marcatori mitocondriali e mitofagici nel tessuto mesencefalico ventrale di topi di 12 mesi. Quantificazione dell'analisi di espressione dei marcatori mitocondriali da Western blot (B-G).

Nella figura 7B-G non sono state riscontrate grandi differenze nei livelli di espressione delle subunità dei complessi I, II e III, ad eccezione del livello di espressione delle subunità del complesso IV.

La figura 7G riporta una diminuzione sostanziale nei topi con *PolgA*<sup>D257A/D257A</sup> rispetto ai topi wild-type, tuttavia questa diminuzione nelle subunità del complesso IV non è stata ulteriormente accentuata dalla perdita di *Parkin*.

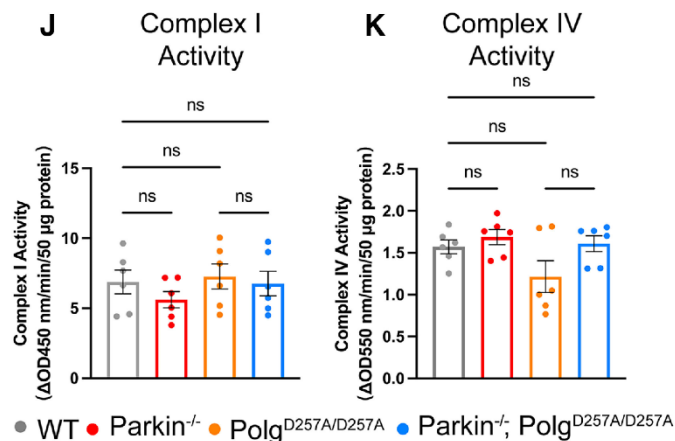


Figura 8 Espressione stazionaria di marcatori mitocondriali e mitofagici nel tessuto mesencefalico ventrale di topi di 12 mesi. Attività del complesso mitocondriale I (J), attività del complesso mitocondriale IV (K).

Le attività dei complessi I e IV non hanno mostrato variazioni significative tra le quattro coorti (Figura 8J e K).

## 2.4 Real-time quantitative PCR

Il numero di copie del mtDNA nel tessuto striatale dei topi è stato determinato tramite Real-time quantitative PCR, utilizzando un pannello di primer per 5 loci diversi del mtDNA, comprendenti *ND4*, *COXI* (6530 e 6620), *CYTB* e *D-loop*. I risultati ottenuti vengono normalizzati col gene *GAPDH*, e poi con i valori wild-type per normalizzare contro l'effetto del campione. Sono stati usati due modelli per analizzare i dati normalizzati: il modello a effetti misti analizza i dati normalizzati presupponendo che tutti i loci analizzati dipendano dal livello di espressione reciproco; il modello ANOVA unidirezionale analizza ciascun locus del mtDNA individualmente.

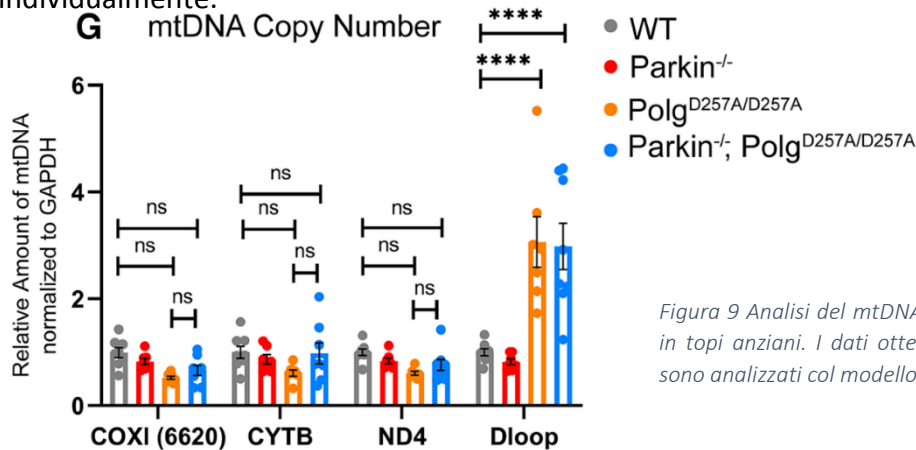


Figura 9 Analisi del mtDNA copy number in topi anziani. I dati ottenuti dalla PCR sono analizzati col modello a effetti misti.

Analizzando i dati ottenuti con modello a effetti misti (Figura 9), il numero di copie del mtDNA non ha rivelato differenze significative considerando *COXI*, *CYTB* o *ND4* tra le coorti.

Tuttavia, nei topi *PolgA<sup>D257A/D257A</sup>* e nei topi *Parkin<sup>-/-</sup>/PolgA<sup>D257A/D257A</sup>* si è riscontrato un accumulo significativo di *D-loop*, ossia della regione che contiene l'origine altamente conservata della replicazione e della trascrizione del mtDNA.

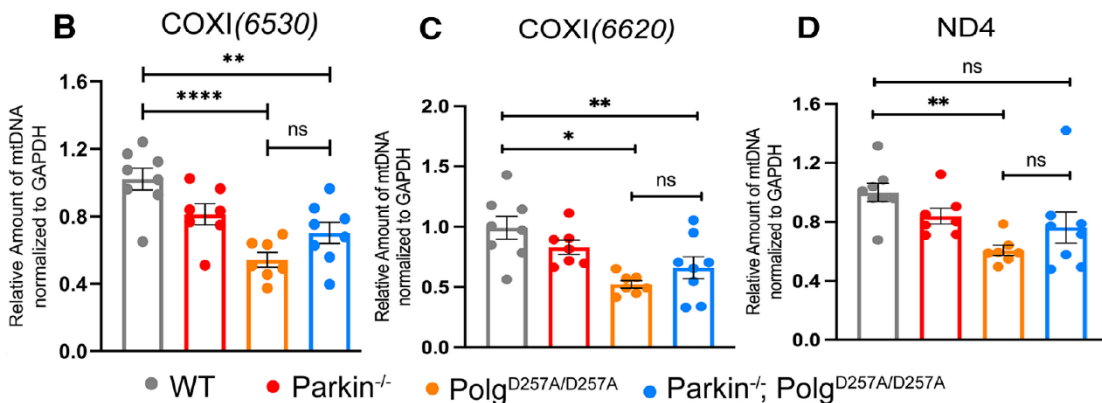


Figura 10 Analisi del mtDNA copy number in topi anziani. I prodotti di PCR del gene *COXI* (6530), *COXI* (6620) e *ND4* sono analizzati con modello ANOVA unidirezionale (B, C, D).

L'analisi ANOVA unidirezionale individuale ha rivelato che i risultati dipendono dai loci: entrambi i set di primer per *COXI* hanno mostrato riduzioni significative del

numero di copie del mtDNA nei topi *PolgA*<sup>D257A/D257A</sup> e nei topi *Parkin*<sup>-/-</sup>/*PolgA*<sup>D257A/D257A</sup> (Figura 10B e C); tuttavia, non esiste differenza statisticamente significativa tra di loro. Si è verificata una sostanziale diminuzione nell'amplificazione di *ND4* nei topi *PolgA*<sup>D257A/D257A</sup> rispetto ai topi selvatici, ma non c'è nessuna differenza statisticamente significativa tra topi *Parkin*<sup>-/-</sup>/*PolgA*<sup>D257A/D257A</sup> e topi selvatici (Figura 10 D).

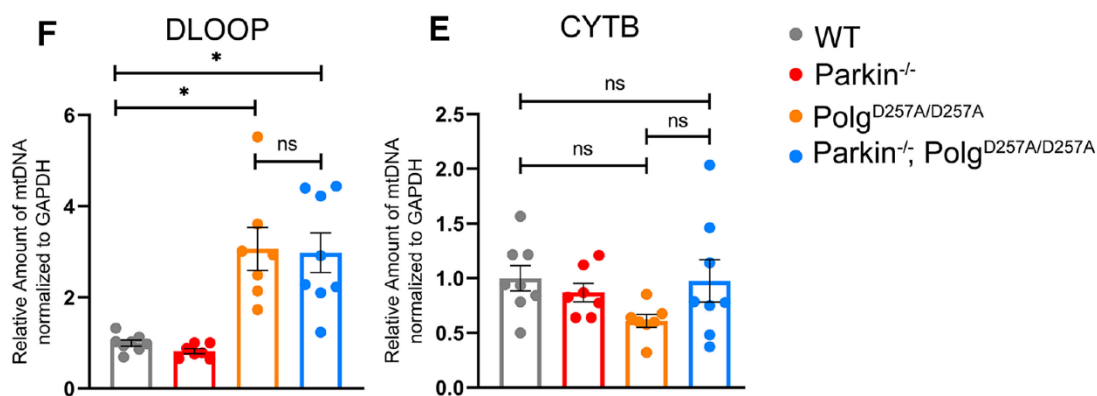


Figura 11 Analisi del mtDNA copy number in topi anziani. I prodotti di PCR del gene D-loop e *CYTB* sono analizzati con modello ANOVA unidirezionale (F, E).

L'analisi ANOVA unidirezionale individuale ha rivelato che non sembravano esserci differenze tra le coorti di topi che utilizzavano primer specifici per *CYTB* (Figura 11E). Inoltre, l'analisi ANOVA unidirezionale ha ulteriormente confermato l'aumento del numero di copie Dloop in tutti i topi con knock-in di *PolgA*<sup>D257A/D257A</sup> (Figura 11F).

Qualunque sia il modello utilizzato, la delezione di *Parkin* non ha alcun effetto evidente sul numero di copie di qualsiasi regione del mtDNA nei topi mutanti *PolgA*.

### 3. Discussione

#### 3.1 Difficoltà a modellizzare la malattia di Parkinson in topo

I topi, in quanto mammiferi, possiedono un'anatomia e una fisiologia relativamente simili a quelle umane, e nel caso dei topi da laboratorio sono stati sviluppati numerosi ceppi transgenici. Tuttavia, nonostante le loro piccole dimensioni, risulta relativamente costoso allevare topi in gran numero, e produrre ceppi transgenici richiede molta manodopera. Gli esseri umani e i topi sono geneticamente molto simili, con valori di similarità pari all'80%. L'eliminazione della funzione *Parkin* nei topi è stata ottenuta mediante la delezione dell'esone 3, dell'esone 7 o dell'esone 2 nel gene *Parkin* [8]. Confrontando questi tre tipi di knockout di *Parkin* si è scoperto che il modello ha dei limiti dovuti all'assenza di perdita di neuroni DA nigro-striatali. Il knockout per l'esone 7 del *Parkin* è l'unico knockout che mostra una perdita neuronale catecolaminergica nel locus coeruleus; la degenerazione in quest'area è una caratteristica della malattia di Parkinson. Confrontando i dati ottenuti tra la condizione wild-type, la mutazione in *Parkin* e/o



la mutazione in *POLG* nello studio in esame [9], [10], si riscontrano sorprendenti somiglianze tra i modelli murini delle diverse coorti, con poche differenze statisticamente significative. Nello studio, il fenotipo da deplezione di *Parkin* è molto tenue; nei topi con knock-out di *Parkin* i marcatori mitofagici sono mantenuti a livelli stazionari, ed il contributo di *Parkin* alla mitofagia sembra molto limitato.

L'autofagia è stata implicata nell'eliminazione del mtDNA dei mammiferi. Il mtDNA paterno è eliminato tramite una modalità attiva; il tal modo il mtDNA viene ereditato esclusivamente per via materna. Nel topo la perdita di *Parkin* o dell'ubiquitina ligasi E3 mitocondriale (*Mul1*) hanno ridotto anche l'efficiente eliminazione dei mitocondri paterni, ma in modo limitato. Tuttavia, il deficit di entrambi ha portato alla ritenzione dei mitocondri paterni; ciò suggerisce che vi siano molteplici meccanismi ridondanti che assicurano la trasmissione del solo mtDNA materno. La fissione mitocondriale è essenziale per la crescita, per la divisione delle cellule e per popolarle con un numero adeguato di mitocondri. Questi risultati suggeriscono che vi siano percorsi compensatori durante lo sviluppo dei topi con carenza di *Parkin*[11]. Rispetto al topo con deficit di *Parkin*, la *Drosophila* con *Parkin* nulla mostra una ridotta durata di vita, difetti locomotori e sterilità maschile [12].

E' possibile che, a causa dell'elevata complessità genetica del topo, geni con effetti ridondanti siano attivati nelle vie di sviluppo e che percorsi alternativi delle proteine funzionali possano compensare la perdita dei loro geni mutati. Sebbene possano essere utili nella ricerca su come curare il Parkinsonismo, tuttavia i modelli murini possono creare difficoltà e ostacoli nel processo di studio della patogenesi. Pertanto, modelli animali con genomi più semplici e caratteristiche *Parkin*-KO più evidenti, come zebrafish o *drosophila*, possono risultare più vantaggiosi rispetto ai topi.

### 3.2 Risultati del Western blot

Esistono rapporti di dipendenza tra i complessi della catena respiratoria complesso I (CI), complesso II (CII) e complesso IV (CIV) nei neuroni della substantia nigra (SN)[7]. La maggior parte dei neuroni della SN ha dimostrato deficit di CI isolato o combinato di CI e CIV, con poche cellule che mostravano perdita selettiva di CIV, deducendo che i deficit di CIV nei neuroni della SN si verificano solo in presenza di deficit CI. Inoltre, l'abbondanza di TFAM e TFB2M (richiesti per la trascrizione delle proteine mitocondriali e la replicazione del mtDNA) nei neuroni nigrali era correlata con i livelli di CI a livello di singola cellula; il livello di TFAM e TFB2M era ridotto nel tessuto con deficit di CI. Nello studio, è stato riscontrato che soltanto il livello di espressione della subunità del CIV presenta diminuzione sostanziale, mentre il livello di espressione della subunità del CI non diminuiva come previsto. L'attività degli enzimi mitocondriali di due complessi evidenzia ulteriormente le

anomalie nel livello di espressione della subunità del CIV; occorrerà trovare o verificare la causa dell'anomalia attraverso esperimenti supplementari.

La subunità del CI, codificata dal nucleo, è un biomarcatore comune negli esseri umani e nei topi; la diminuzione di CI è stata rilevata tramite le proteine NDUFB8 o NDUFA13 (entrambe codificate dal nucleo) [7]. Pertanto, nel caso in cui la diminuzione di CI sia rilevabile, ciò è indipendente dal fatto che per il test venga utilizzata una proteina codificante mitocondriale o nucleare. Possiamo ulteriormente verificare la riduzione del CI tramite l'abbondanza di TFAM e TFB2M con Western Blot. Inoltre, una riduzione significativa di una subunità di CIV codificata dai mitocondri, se dovuta all'accumulo di delezioni del mtDNA, può essere verificata tramite test RT-PCR.

Poiché PINK/Parkin svolge un ruolo importante nel controllo della qualità mitocondriale, degradando PARIS per promuovere la biogenesi mitocondriale, è essenziale effettuare il rilevamento di PARIS e PGC-1 $\alpha$ .

### 3.3 Test di deficit non motori

Clinicamente, la malattia di Parkinson umana non viene diagnosticata finché non si sviluppano deficit motori (i sintomi cardinali di Parkinson). La malattia di Parkinson di solito non viene diagnosticata fino a quando oltre l'80% dell'innervazione dopaminergica striatale, i neuroni nella SNpc, muoiono e i livelli di dopamina nello striato diminuiscono portando alla conseguente perdita del controllo motorio volontario del paziente [13]. I sintomi motori presentano un certo grado di ritardo rispetto ai sintomi non motori, che possono comparire anni, a volte decenni, prima dell'esordio del fenotipo motorio. Nello studio questo fenomeno è stato verificato a livello molecolare: i neuroni nel bulbo olfattivo sembrano più sensibili alla disfunzione mitocondriale; presentano non soltanto la diminuzione del livello della dopamina ma anche la disregolazione delle catecolamine e dell'indolamina. Pertanto, considerata la disregolazione delle catecolamine già verificata nel bulbo olfattivo, è essenziale aggiungere un test non motorio (buried pellet test) ai test comportamentali; nello studio, i test comportamentali comprendevano solo test motori come Pole test, Openfield e Grip strength.

I disturbi olfattivi sono uno dei primi sintomi non motori osservati nella malattia di Parkinson.

I pazienti con malattia di Parkinson hanno dimostrato compromissioni nel rilevamento, nella differenziazione e nell'identificazione degli odori. Per misurare la funzione olfattiva generale del modello di topo, è possibile utilizzare il buried pellet test [13]. Esso si basa sulla localizzazione da parte del topo di un oggetto nascosto tramite l'odore. I test comportamentali dell'olfatto possono facilitare una diagnosi precoce della malattia di Parkinson, poiché l'alterazione dell'olfatto

è stata correlata positivamente con un aumento del rischio di sviluppare la malattia.

### 3.4 Risultati della Quantitative PCR

Gli esperimenti di immunohistochimica, HPLC e WB hanno mostrato una serie di effetti derivanti dalla perdita di Parkin endogena in abbinamento alla disfunzione mitocondriale *PolgA*<sup>D257A/D257A</sup>. Tuttavia, se si vuole studiare in modo sostanziale l'effetto di questi geni sulla funzione mitocondriale, è opportuno quantificare il numero relativo di copie del mtDNA per mitocondrio e la delezione di mtDNA. Il DNA mitocondriale è una molecola circolare di 16.569 bp di DNA a doppio filamento contenente 37 geni che specificano: 13 polipeptidi, 22 RNA di trasferimento (tRNA) e 2 RNA ribosomiali (rRNA). Tutti i 13 polipeptidi sono componenti del sistema di fosforilazione ossidativa che genera ATP: sette sono subunità del complesso I (*ND1-ND6, ND4L*), uno è una subunità del complesso III (*cyt b*), tre sono subunità del complesso IV (*COX I-COX III*) e due sono subunità del complesso V (ATPasi 6 e ATPasi 8). Ciascuno di questi quattro complessi contiene altre subunità codificate da geni nucleari; tutte le altre proteine situate nei mitocondri, comprese tutte le subunità del complesso II, sono codificate esclusivamente dal genoma nucleare [14]. Un singolo mitocondrio contiene copie multiple (2-10) di DNA mitocondriale. Copie contenenti mutazioni (es: delezioni) e copie non-mutate (wild-type) possono coesistere nello stesso mitocondrio; la condizione è detta eteroplasmia. Al contrario, nell'omoplasmia tutte le copie sono selvatiche. Poiché il mtDNA è presente in copie multiple all'interno della cellula, le mutazioni di solito non sono immediatamente fatali per le cellule, poiché il mtDNA wild-type può parzialmente compensare i geni difettosi o assenti dal mtDNA mutato (controllo di qualità mitocondriale) [15]. Oltre al controllo della qualità mitocondriale, a livello mitocondriale esistono meccanismi compensatori di guadagno di funzione, tra cui un aumento del numero di copie del mtDNA per mitocondrio e un potenziamento della rete di creste mitocondriali associata a OPA1, consentendo ai neuroni dopaminergici della SNpc di sopportare alti livelli di delezioni del DNA mitocondriale (fino al 60%) senza diffusi danni funzionali o strutturali [16]. Il controllo della qualità mitocondriale e i meccanismi compensatori avvengono per ciascuna unità cellulare, pertanto nelle analisi dobbiamo normalizzare i dati con un gene housekeeping codificato nel nucleo, come *GAPDH*, actina beta (*ACTB*) o *ANG1*.

#### 3.4.1 Numero di copie di mtDNA e delezione del mtDNA

Per quantificare in modo affidabile la quantità di mtDNA si procede tramite analisi in due diverse loci (*ND1* e *ND4*) del genoma mitocondriale con RT-PCR.

Il locus *ND1* viene raramente deletto (è presente nel genoma rimanendo nel 94% dei casi con delezioni singole e nel 100% dei casi con delezioni multiple del mtDNA). Il locus *ND4* viene invece deletto con alta frequenza (82% dei casi con una delezione singola su larga scala e 96% dei casi con delezioni multiple del mtDNA). I valori Ct

possono essere utilizzati come misura del DNA input e per quantificare la quantità relativa di *ND1* a *ND4* con la seguente equazione:  $R = 2^{-\Delta Ct}$ , dove R rappresenta il numero di copie relative calcolato e  $\Delta Ct = Ct_{ND1} - Ct_{ND4}$  [15]. Il numero relativo di copie del DNA mitocondriale nella coorte corrispondente viene determinato dalla quantità più alta tra i geni dei diversi loci (di solito è il locus *ND1*). I livelli di delezione in una coorte corrispondente sono stati calcolati con tutte le possibili combinazioni tra rapporti genici tranne il *D-loop* e registrando i livelli massimi di delezione [16]. Un altro metodo per valutare le delezioni del mtDNA utilizza la Long-range PCR (LPCR) [16], in cui l'estensione operata dalla DNA polimerasi è interrotta dalla delezione sul DNA. Il mtDNA non deletato e mutato sono analizzati tramite Southern blot. I prodotti amplificati dal LPCR sono separati attraverso gel di agarosio allo 0,8% contenente bromuro di etidio e visualizzati tramite luce UV. Il mtDNA non contenente delezioni è amplificato con lunghezza piena tra due primer utilizzati e forma un'unica banda luminosa sul gel di agarosio, mentre i mtDNA contenenti delezioni generano frammenti più piccoli di quelli a lunghezza piena (Figura 13 *WT/WT* e *WT/D257A*), formano delle sbavature sul gel (Figura 13 *D257A/D257A*).

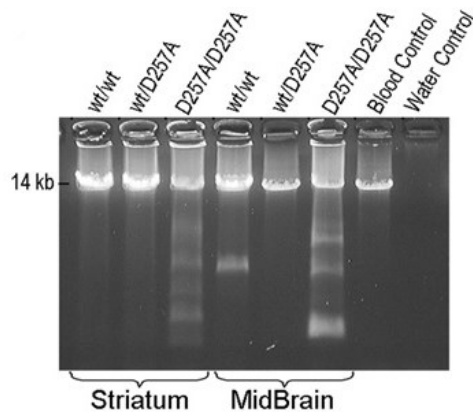


Figura 12 Individuazione di delezioni nel mtDNA tramite long-range PCR in campioni di mesencefalo e striato di topi omozigoti *POLGD257A* (*D257A/D257A*), eterozigoti (*D257A/wt*) e wild-type (*wt/wt*) [15].

### 3.4.2 La diminuzione di *COXI*

Sperimentalmente, non è un approccio del tutto corretto valutare il numero di mitocondri per cellula in una data quantità di tessuto mediante il numero di copie del mtDNA, soprattutto in presenza di mutazioni di *PRKN* e/o *POLG*. Non esiste infatti una netta correlazione tra l'abbondanza di mtDNA e l'abbondanza di mitocondri nei neuroni DA [9]. La massa mitocondriale è determinata tramite la quantificazione della proteina Porin o VDAC sui mitocondri [9] [16]. La quantificazione di VDAC nello studio ha rivelato che relativamente alla massa mitocondriale non c'è nessuna differenza tra le coorti. In effetti, non è un criterio del tutto corretto utilizzare il numero assoluto di geni in siti diversi come stima del numero relativo di copie del mtDNA. Esistono infatti meccanismi compensatori che aumentano il numero di copie del mtDNA per mitocondrio [16].

Ad esempio, il numero assoluto di *ND4* diminuisce soltanto nella coorte di *PolgA<sup>D257A/D257A</sup>*, mentre nel topo con *Parkin<sup>-/-</sup>/PolgA<sup>D257A/D257A</sup>* il meccanismo compensatorio è attivato ed il numero di mtDNA aumenta.

I dati ottenuti mediante RT-PCR sono stati utilizzati soltanto per confrontare i livelli di espressione genica nello stesso locus tra coorti, come nel caso della riduzione di *COXI*. Sulla base dei dati di RT-PCR, la subunità del complesso IV era significativamente ridotta nel Southern blot, il che potrebbe essere dovuto all'accumulo di delezioni nel locus *COXI*.

#### 3.4.3 L'aumento del *D-loop*

Il rapporto tra locus *D-loop* e locus *ND1* (numero relativo di copie del mtDNA) rappresenta lo stato di replicazione del mtDNA; un rapporto più elevato rappresenta molecole di mtDNA trascritte o replicate più attivamente [7]. Il risultato più interessata nello studio è stato l'aumento notevole nel numero assoluto della regione *D-loop*. Il rapporto tra *D-loop* e copie del mtDNA è molto alto; si ipotizza che nel meccanismo di compensazione possa esserci non solo la replicazione del mtDNA, ma anche una specifica amplificazione del *D-loop* per aumentare la trascrizione e la replicazione mitocondriale.

## 4. Conclusioni

Il topo non è un organismo modello del tutto fedele per fenocopiare il Parkinsonismo. Lo zebrafish o la drosophila possono rappresentare delle opzioni migliori del topo, sulla base della compensazione della perdita di Parkin riscontrata nel topo. I test non motori, aggiunti agli esperimenti con test comportamentali, dovrebbero essere dei test prioritari; i sintomi non motori della malattia di Parkinson sono caratterizzati da esordio precoce e i neuroni correlati hanno elevata sensibilità alla mutazione del mtDNA. La disregolazione della DA può essere monitorata non soltanto rilevando la concentrazione di DA mediante HPLC ma anche calcolando il proprio tasso di turnover. Sono importanti la validazione e la quantificazione delle diverse subunità del complesso della catena respiratoria e dei marcatori mitofagici, ma anche di quelle proteine che regolano l'espressione di subunità complesse come TFAM, e di quelle regolate da Parkin, come PARIS e PGC-1 $\alpha$ . La delezione del mtDNA viene valutata tramite il LPCR o il rapporto tra i prodotti di PCR di geni localizzati in diversi loci sul mtDNA; *ND1* è un locus essenziale per determinare il numero relativo di copie del mtDNA per mitocondrio.

## 5. Bibliografia

- [1] Simon D K, Tanner C M and Brundin P 2020 Parkinson Disease Epidemiology, Pathology, Genetics and Pathophysiology *Clin Geriatr Med* **36** 1–12
- [2] Panicker N, Ge P, Dawson V L and Dawson T M 2021 The cell biology of Parkinson's disease *J Cell Biol* **220** e202012095
- [3] Pickrell A M and Youle R J 2015 The Roles of PINK1, Parkin and Mitochondrial Fidelity in Parkinson's Disease *Neuron* **85** 257–73
- [4] Stevens D A, Lee Y, Kang H C, Lee B D, Lee Y-I, Bower A, Jiang H, Kang S-U, Andrabi S A, Dawson V L, Shin J-H and Dawson T M 2015 Parkin loss leads to PARIS-dependent declines in mitochondrial mass and respiration *Proc Natl Acad Sci U S A* **112** 11696–701
- [5] Gustafson M A, Sullivan E D and Copeland W C 2020 Consequences of Compromised Mitochondrial Genome Integrity *DNA Repair (Amst)* **93** 102916
- [6] Grünewald A, Rygiel K A, Hepplewhite P D, Morris C M, Picard M and Turnbull D M 2016 Mitochondrial DNA Depletion in Respiratory Chain–Deficient Parkinson Disease Neurons *Ann Neurol* **79** 366–78
- [7] Fleming S M, Fernagut P-O and Chesselet M-F 2005 Genetic Mouse Models of Parkinsonism: Strengths and Limitations *NeuroRx* **2** 495–503
- [8] Pinto M, Nissanka N and Moraes C T 2018 Lack of Parkin Anticipates the Phenotype and Affects Mitochondrial Morphology and mtDNA Levels in a Mouse Model of Parkinson's Disease *J Neurosci* **38** 1042–53
- [9] Pickrell A M, Huang C-H, Kennedy S R, Ordureau A, Sideris D P, Hoekstra J G, Harper J W and Youle R J 2015 Endogenous Parkin Preserves Dopaminergic Substantia Nigral Neurons following Mitochondrial DNA Mutagenic Stress *Neuron* **87** 371–81
- [10] Pickles S, Vigié P and Youle R J 2018 The art of mitochondrial maintenance *Curr Biol* **28** R170–85
- [11] Greene J C, Whitworth A J, Kuo I, Andrews L A, Feany M B and Pallanck L J 2003 Mitochondrial pathology and apoptotic muscle degeneration in *Drosophila parkin* mutants *Proc Natl Acad Sci U S A* **100** 4078–83






- [12] Taylor T N, Greene J G and Miller G W 2010 Behavioral phenotyping of mouse models of Parkinson's Disease *Behav Brain Res* **211** 1–10
- [13] Moraes C T, Atencio D P, Oca-Cossio J and Diaz F 2003 Techniques and Pitfalls in the Detection of Pathogenic Mitochondrial DNA Mutations *The Journal of molecular diagnostics : JMD* **5** 197
- [14] He L, Chinnery P F, Durham S E, Blakely E L, Wardell T M, Borthwick G M, Taylor R W and Turnbull D M 2002 Detection and quantification of mitochondrial DNA deletions in individual cells by real-time PCR *Nucleic Acids Res* **30** e68
- [15] Perier C, Bender A, García-Arumí E, Melià M J, Bové J, Laub C, Klopstock T, Elstner M, Mounsey R B, Teismann P, Prolla T, Andreu A L and Vila M 2013 Accumulation of mitochondrial DNA deletions within dopaminergic neurons triggers neuroprotective mechanisms *Brain* **136** 2369–78

## 6. Appendice

Di seguito viene allegato l'articolo oggetto della precedente discussione.

Scott L, Karuppagounder S S, Neifert S, Kang B G, Wang H, Dawson V L and Dawson T M 2022 The Absence of Parkin Does Not Promote Dopamine or Mitochondrial Dysfunction in PolgAD257A/D257A Mitochondrial Mutator Mice *J Neurosci* **42** 9263–77

# The Absence of Parkin Does Not Promote Dopamine or Mitochondrial Dysfunction in PolgA<sup>D257A/D257A</sup> Mitochondrial Mutator Mice

Laura Scott,<sup>1,2,3</sup>  Senthilkumar S. Karuppagounder,<sup>1,4</sup>  Stewart Neifert,<sup>1,3,4</sup>  Bong Gu Kang,<sup>1,4</sup> Hu Wang,<sup>1,4</sup>  Valina L. Dawson,<sup>1,2,3,4,5,6\*</sup> and  Ted M. Dawson<sup>1,2,3,4,5,7\*</sup>

<sup>1</sup>Neuroregeneration and Stem Cell Programs, Institute for Cell Engineering, Johns Hopkins University School of Medicine, Baltimore, Maryland 21205, <sup>2</sup>Cellular and Molecular Medicine Program, Johns Hopkins University School of Medicine, Baltimore, Maryland 21205, <sup>3</sup>Adrienne Helis Malvin Medical Research Foundation, New Orleans, Louisiana 70130-2685, <sup>4</sup>Department of Neurology, Johns Hopkins University School of Medicine, Baltimore, Maryland 21205, <sup>5</sup>Solomon H. Snyder Department of Neuroscience, Johns Hopkins University School of Medicine, Baltimore, Maryland 21205, <sup>6</sup>Department of Physiology, Johns Hopkins University School of Medicine, Baltimore, Maryland 21205, and <sup>7</sup>Department of Pharmacology and Molecular Sciences, Johns Hopkins University School of Medicine, Baltimore, Maryland 21205

Parkinson's disease (PD) is characterized by the progressive loss of dopaminergic neurons in the substantia nigra pars compacta (SNpc). In this study, we generated a transgenic model by crossing germline Parkin<sup>-/-</sup> mice with PolgA<sup>D257A</sup> mice, an established model of premature aging and mitochondrial stress. We hypothesized that loss of Parkin<sup>-/-</sup> in PolgA<sup>D257A/D257A</sup> mice would exacerbate mitochondrial dysfunction, leading to loss of dopamine neurons and nigral-striatal specific neurobehavioral motor dysfunction. We found that aged Parkin<sup>-/-</sup>/PolgA<sup>D257A/D257A</sup> male and female mice exhibited severe behavioral deficits, nonspecific to the nigral-striatal pathway, with neither dopaminergic neurodegeneration nor reductions in striatal dopamine. We saw no difference in expression levels of nuclear-encoded subunits of mitochondrial markers and mitochondrial Complex I and IV activities, although we did observe substantial reductions in mitochondrial-encoded COX4I1, indicating mitochondrial dysfunction as a result of PolgA<sup>D257A/D257A</sup> mtDNA mutations. Expression levels of mitophagy markers LC3I/LC3II remained unchanged between cohorts, suggesting no overt mitophagy defects. Expression levels of the parkin substrates, VDAC, NLRP3, and AIMP2 remained unchanged, suggesting no parkin dysfunction. In summary, we were unable to observe dopaminergic neurodegeneration with corresponding nigral-striatal neurobehavioral deficits, nor Parkin or mitochondrial dysfunction in Parkin<sup>-/-</sup>/PolgA<sup>D257A/D257A</sup> mice. These findings support a lack of synergism of Parkin loss on mitochondrial dysfunction in mouse models of mitochondrial deficits.

**Key words:** mitochondria; mitophagy; parkin; Parkinson's disease; POLG

## Significance Statement

Producing a mouse model of Parkinson's disease (PD) that is etiologically relevant, recapitulates clinical hallmarks, and exhibits reproducible results is crucial to understanding the underlying pathology and in developing disease-modifying therapies. Here, we show that Parkin<sup>-/-</sup>/PolgA<sup>D257A/D257A</sup> mice, a previously reported PD mouse model, fails to reproduce a Parkinsonian phenotype. We show that these mice do not display dopaminergic neurodegeneration nor nigral-striatal-dependent motor deficits. Furthermore, we report that Parkin loss does not synergize with mitochondrial dysfunction. Our results demonstrate that Parkin<sup>-/-</sup>/PolgA<sup>D257A/D257A</sup> mice are not a reliable model for PD and adds to a growing body of work demonstrating that Parkin loss does not synergize with mitochondrial dysfunction in mouse models of mitochondrial deficits.

Received Mar. 17, 2022; revised Oct. 10, 2022; accepted Oct. 16, 2022.

Author contributions: L.S., V.L.D., and T.M.D. designed research; L.S., S.S.K., S.N., B.G.K., and H.W. performed research; V.L.D. and T.M.D. contributed unpublished reagents/analytic tools; L.S., S.S.K., S.N., B.G.K., H.W., V.L.D., and T.M.D. analyzed data; L.S. wrote the first draft of the paper; L.S., S.S.K., S.N., H.W., V.L.D., and T.M.D. edited the paper; V.L.D. and T.M.D. wrote the paper.

This work was supported by the National Institutes of Health/National Institute of Neurological Disorders and Stroke Grant P50 NS38377 and the JPB Foundation. T.M.D. is the Leonard and Madlyn Abramson Professor in Neurodegenerative Diseases. V.L.D. and T.M.D. acknowledge the joint participation by the Adrienne Helis Malvin Medical Research Foundation through its direct engagement in the continuous active conduct of medical research in conjunction with the Johns

Hopkins Hospital and the Johns Hopkins University School of Medicine and the Foundation's Parkinson's Disease Program M-2014, M-2016. This work was also supported by the National Science Foundation under Grant 2017238665 (to L.S.).

\*V.L.D. and T.M.D. contributed equally to this work.

The authors declare no competing financial interests.

Correspondence should be addressed to Valina L. Dawson at vdawson@jhmi.edu or Ted M. Dawson at tdawson@jhmi.edu..

<https://doi.org/10.1523/JNEUROSCI.0545-22.2022>

Copyright © 2022 the authors



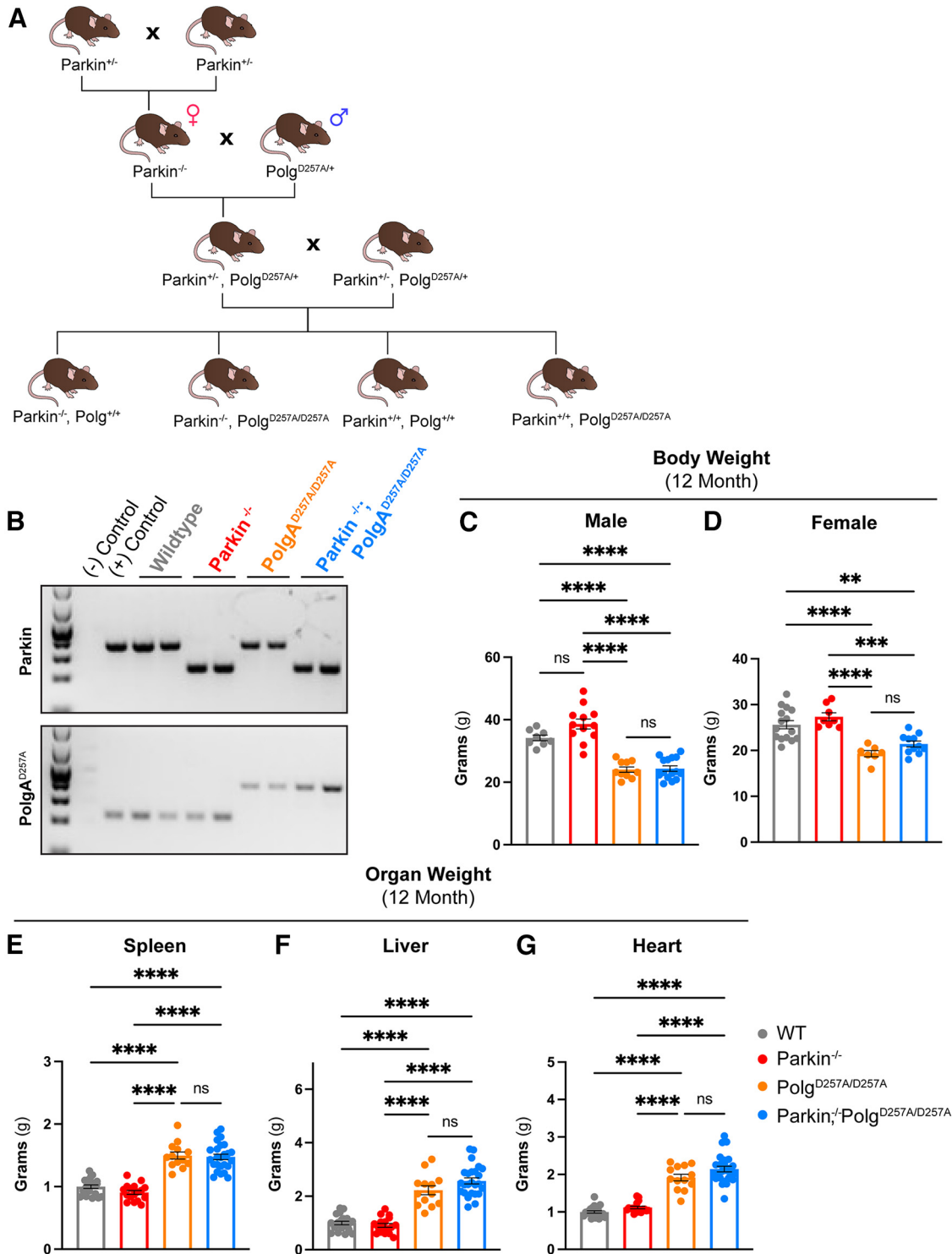


**Figure 1.** Physiologic data of 12-month-old mice. **A**, Schematic depicting breeding scheme to produce  $Parkin^{-/-}/PolgA^{D257A/D257A}$  mice. Female and male mice are depicted with the symbol for females and males respectively. **B**, Representative gel confirming genotypes of pups. **C**, **D**, Body weight of 12-month-old female and male mice. Results are the mean  $\pm$  SEM,  $n = 7-15$  per group. Datasets were unbiasedly analyzed using ROUT outlier analysis with a maximum false discovery rate ( $q$ ) of 0.1%. Data were found to be normally distributed via D’Agostino and Pearson test. SDs did not significantly differ per Brown–Forsythe test of variance. Significance of means was analyzed via ordinary one-way ANOVA (**C**:  $F_{(3,41)} = 40.94$  \*\*\*\* $p < 0.0001$ ; **D**:  $F_{(5,37)} = 15.97$  \*\*\*\* $p < 0.0001$ ). *Post hoc* Tukey’s test resulted in \*\*\*\* $p < 0.0001$  for all  $PolgA^{D257A/D257A}$ -expressing mice compared with wild-type and  $Parkin^{-/-}$  for both male and female cohorts, ns, not significant. **E**, **F**, Mass of spleen and liver (organs with known defects in  $PolgA^{D257A/D257A}$  mice) were recorded. Mass was normalized to body weight and then further normalized to the average wild-type organ mass/body weight ratio. Results are the mean  $\pm$  SEM,  $n = 14-25$  per group. Datasets were unbiasedly analyzed using ROUT outlier analysis with a maximum false discovery rate ( $q$ ) of 0.1%. Data were found to be normally distributed via D’Agostino and Pearson test. Brown–Forsythe test of variance found that SDs differed significantly; therefore, significance of means was determined via a Welch one-way ANOVA (**E**:  $W_{(5,37)} = 65.89$  \*\*\*\* $p < 0.0001$ ; **F**:  $W_{(3,43.85)} = 93.922$  \*\*\*\* $p < 0.0001$ ). *Post hoc* Dunnett’s T3 test resulted in **E**: \*\*\*\* $p < 0.0001$  for all  $PolgA^{D257A/D257A}$ -expressing mice compared with wild-type and  $Parkin^{-/-}$ ; **F**: \*\*\*\* $p < 0.0001$  for all  $PolgA^{D257A/D257A}$ -expressing mice compared with wild-type and  $Parkin^{-/-}$ , ns, not significant. **G**, Mass of hearts were recorded. Mass was normalized to body weight and then further normalized to the average wild-type organ mass/body weight ratio. Results are the mean  $\pm$  SEM,  $n = 14-25$  per group. Datasets were unbiasedly analyzed using ROUT outlier analysis with

## Introduction

Parkinson's disease (PD) is a progressive neurodegenerative disease characterized by the degeneration of dopamine neurons in the substantia nigra pars compacta (SNpc). Although a sporadic disease, mutations encoding the gene for the E3 ligase Parkin result in the second most common form of familial PD (Kitada et al., 1998; Bonifati, 2014). Data suggests that mutations in PRKN result in abnormal mitochondrial quality control, pointing to deficits in mitophagy, fission/fusion, transport, and/or biogenesis (Ge et al., 2020). The relative contributions of each arm of the mitochondrial quality control to dopamine cell death in PD is an area of active investigation (Grenier et al., 2013; Ge et al., 2020; Panicker et al., 2021).

We have previously reported that adult conditional Parkin<sup>-/-</sup> mice exhibit dopamine neurodegeneration, motor deficits, and abnormal mitochondria morphology and function. We further linked the loss of Parkin to the accumulation of PARIS, a Parkin substrate, which was found to suppress regulators of mitochondrial biogenesis (Shin et al., 2011; Pirooznia et al., 2020). Interestingly, germline Parkin knock-out (KO) mice (Parkin<sup>-/-</sup>) lack an obvious PD phenotype and corresponding dopaminergic loss (Fleming et al., 2005; Perez and Palmiter, 2005). In an effort to generate a mouse model of PD that does not stereotaxically or pharmacologically target dopaminergic neurons, thus a more etiologically relevant model, we generated a double transgenic line by crossing germline Parkin<sup>-/-</sup> mice with the mitochondrial DNA (mtDNA) PolgA D257A mice (PolgA<sup>+/D257A</sup>), a model of mitochondrial dysfunction and premature aging similar to a prior report (Pickrell et al., 2015). PolgA<sup>D257A/D257A</sup> mice display a progressive accumulation of mtDNA mutations, resulting in a reduction in oxidative phosphorylation (OXPHOS) function and a significantly shortened lifespan (Kujoth et al., 2005).

We initially generated the Parkin<sup>-/-</sup>/PolgA<sup>D257A/D257A</sup> double transgenic mouse model to better understand the role of mitochondrial quality control and the contributions of defects in mitophagy versus mitochondrial biogenesis in promoting dopaminergic neurodegeneration because it had been reported that the Parkin<sup>-/-</sup>/PolgA<sup>D257A/D257A</sup> mice exhibited loss of dopamine neurons and that the absence of Parkin in PolgA<sup>D257A/D257A</sup> mice lead to enhanced motor deficits and mitochondrial dysfunction (Pickrell et al., 2015). We hypothesized that deficits in mitochondrial biogenesis would predominate over deficits in mitophagy. To test our hypothesis we used behavioral, metabolic, and biochemical assessments in Parkin<sup>-/-</sup>/PolgA<sup>D257A/D257A</sup>; PolgA<sup>D257A/D257A</sup>, Parkin<sup>-/-</sup>, and wild-type (WT) littermate controls.

## Materials and Methods

### Animals

PolgA<sup>D257A/D257A</sup> mice were previously reported (Kujoth et al., 2005) and were obtained from The Jackson Laboratory: B6.129S7 (Cg)-Polgtm1TproI/J). Mice were genotyped with primer set: PolgA\_F 5'-TCCACTGAGGGAGCTTCTGT-3' and PolgA\_R 5'-CTTCC

CTAAAGACCGCAGGG-3'. Using these primers allowed for the amplification of the, knock-in allele, resulting in a positive band that was 171-bp higher than the wild-type band. These results were confirmed via sequencing. Parkin<sup>-/-</sup> mice were used as previously described (Von Coelln et al., 2004) in which exon 7 was deleted, generating a catalytically null mutant. All mice were backcrossed to C57Bl/6 mice (Charles River) for at least 10 generations. The four genotypes of mice used in this study were WT (Parkin<sup>+/+</sup>/PolgA<sup>+/+</sup>), Parkin<sup>-/-</sup>, PolgA<sup>D257A/D257A</sup>, and Parkin<sup>-/-</sup>/PolgA<sup>D257A/D257A</sup>. Animals were housed in a climate-controlled room with a 12/12 h light/dark cycle. Mice were given unlimited access to food and water. Both male and female mice were used.

### Pole test

The pole test was performed as previously published (Ogawa et al., 1985; Matsuura et al., 1997) with slight modifications. Briefly, the mouse was placed face-up on top of a wrapped metal pole (diameter 8 mm; height 55 cm). To familiarize the mouse to its new environment, a tray with cage bedding was placed at the bottom of the pole. Each mouse was trained for 3 d. On the fourth day, the mouse was subjected to timed trials that were video recorded. Because of large variability trials, each mouse performed five trials, with a minimum of 1 min of rest in between each trial set. The time it took for the mouse to turn around and descend the pole was recorded. The mouse was given 120 s to turn and 120 s to descend the pole, giving each trial a maximum value of 240 s. If the mouse failed to turn in 120 s, the rater manually turned the mouse and started the clock, again recording the time of descent until a maximum of 120 s. If the mouse fell, it was given a maximum score of 120 s for descent. An average of all five trials was used with the total trial time (latency plus descent) used for analysis.

### Openfield

The Photobeam Activity System (PAS)-Openfield suite from San Diego Instruments was used in the Johns Hopkins University School of Medicine Animal Behavior Core. Raters were trained in the use of the equipment, and equipment and animal handling were conducted per manufacturer and behavioral core protocol, respectively. Briefly, animals were brought into the suite for acclimation 1 h before testing. Each station was wiped down with 10% bleach before use. At the beginning of the testing period, each mouse was placed in the middle of the 16 × 16-inch photobeam box. The testing period concluded at the end of 15 min. Mice were placed back in their cages and each station was cleaned.

### Grip strength

The Grip Strength Test from BIOSEB was used according to the manufacturer's protocol. Mice were trained 1 d before testing. In brief, mice were held by the tail and their forelimbs were allowed to grip the mesh strength plate. Mice were gently pulled backwards, away from the meter, in a horizontal plane. The force applied to the grid at peak tension (the point before the mouse lost its grip) was recorded in grams. The same protocol was used to determine hindlimb strength, although in this test the mouse was allowed to grip the grid with both its forelimbs and hindlimbs, giving a reading of total limb strength. Force readings were normalized to body weight for analysis.

### Immunohistochemistry

Mice were perfused with ice cold 1 × PBS (Quality Biologicals, pH 7.4), and the brains were dissected from the skulls. The left hemisphere was immediately placed in a 15-ml conical tube (Falcon) with cold 4% paraformaldehyde/PBS (Santa Cruz, pH 7.4). Conical tubes were placed on a rotator overnight at 4°C. After fixation, the 4% paraformaldehyde/PBS solution was replaced with cryoprotective 30% sucrose/PBS (pH 7.4) and continued to rotate at 4°C until the brains migrated to the bottom of the conical tubes. Brains were frozen at -80°C and then were cut in serial coronal sections (30-μm sections throughout the entire brain) using a HM440E microtome (Microm). Free floating sections were collected in a 12-well plate (Falcon), allowing for the collections of four complete z-stacks per brain. Sections were blocked with a 10% goat serum/PBS/0.2% Triton X-100 solution for 1 h and then incubated with a primary

←

a maximum false discovery rate (q) of 0.1%. Data were found to be normally distributed via D'Agostino and Pearson test. SDs for heart mass did not significantly differ. Significance of means was analyzed via an ordinary one-way ANOVA ( $G: F_{(3,71)} = 55.26$ , \*\*\*\* $p < 0.0001$ ). *Post hoc* Tukey's test resulted \*\*\*\* $p < 0.0001$  for all PolgA<sup>D257A/D257A</sup>-expressing mice compared with wild-type and Parkin<sup>-/-</sup>, ns, not significant. Analysis and graphs were produced using GraphPad Prism 8.4.3.

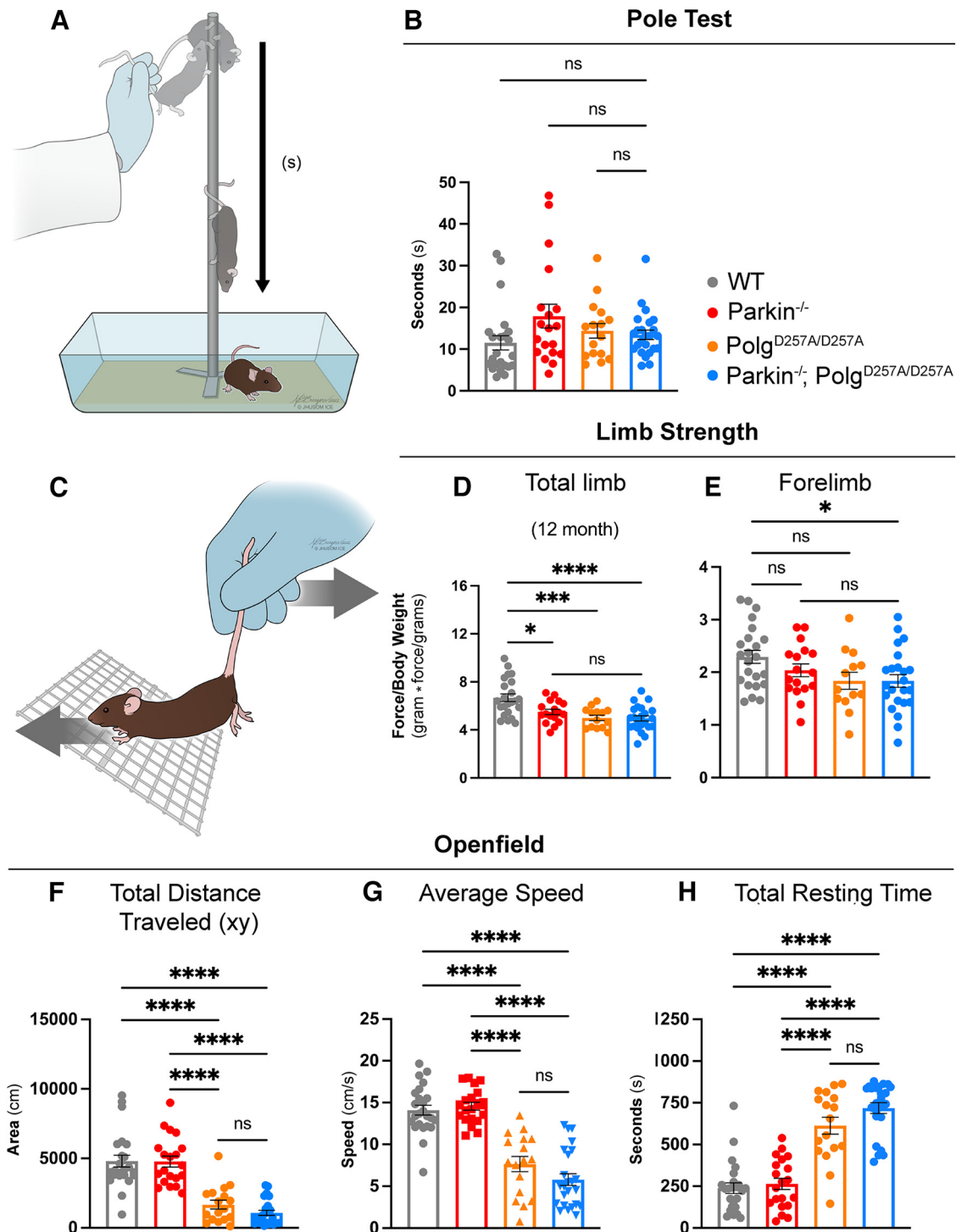


**Figure 2.** Behavioral and neuromuscular data of 12-month-old mice. **A**, Schematic of the pole test. **B**, Latency values of pole test of 12-month-old mice. Results are the median  $\pm$  SEM,  $n = 17$ –25 per group with an average of five trials per mouse used for analysis. Datasets were unbiasedly analyzed using ROUT outlier analysis with a maximum false discovery rate ( $q$ ) of 0.1%. Data were found to be non-normally distributed via D’Agostino and Pearson test (with two out of the four groups being found to be non-normally distributed). Significance of medians was analyzed via Kruskal–Wallis nonparametric ANOVA ( $KW(4,82) = 7.271, p = 0.0637$ ). *Post hoc* Kruskal–Wallis test for multiple comparisons resulted in no significant differences (ns) between groups. **C**, Schematic depicting directionality of force (mouse) versus tester in grip strength testing. **D**, **E**, Total limb and forelimb strength (in gram\*force) normalized to body weight (grams). Results are the mean  $\pm$  SEM,  $n = 13$ –23 per group. Datasets were unbiasedly analyzed using ROUT outlier analysis with a maximum false discovery rate ( $q$ ) of 0.1%. Data were found to be normally distributed via D’Agostino and Pearson test. Brown–Forsythe test of variance found no difference in SDs. Significance of means was analyzed via an ordinary one-way ANOVA (**D**:  $F_{(3,73)} = 10.21$  \*\*\*\* $p < 0.0001$ ; **E**:  $F_{(3,72)} = 3.012$  \* $p = 0.0536$ ). *Post hoc* Tukey’s test was performed and resulted in **D**: \* $p = 0.0117$  for wild-type versus  $Parkin^{-/-}$ , \*\*\*\* $p = 0.0003$  for wild-type versus  $PolgA^{D257A/D257A}$ , and \*\*\*\* $p < 0.0001$  for wild-type versus  $Parkin^{-/-}/PolgA^{D257A/D257A}$ ; **E**: \* $p = 0.0398$  for wild-type versus  $Parkin^{-/-}/PolgA^{D257A/D257A}$ , ns, not significant. Forelimb and total limb strength at three, six, and nine months is provided in Extended Data Figure 2-1. **F**, Openfield data analyzing total distance traveled in the xy direction during the 15-min testing period. Results are the mean  $\pm$  SEM,  $n = 17$ –24 per group. Datasets were unbiasedly analyzed using ROUT outlier analysis with a maximum false discovery rate ( $q$ ) of 0.1%. Data were found to be normally distributed via D’Agostino and Pearson test. SDs were found to differ significantly per Brown–Forsythe test of variance. Therefore, significance of means was analyzed via a Welch one-way ANOVA ( $W(5,0,51.85) = 36.71$  \*\*\*\* $p < 0.0001$ ). *Post hoc* Dunnett’s T3 test resulted in \*\*\*\* $p < 0.0001$  for wild-type versus all  $PolgA^{D257A/D257A}$ -expressing mice and for  $Parkin^{-/-}$  versus all  $PolgA^{D257A/D257A}$ -expressing mice. **G**, Average speed of locomotion during 15-min test period. Results are the mean  $\pm$  SEM,  $n = 17$ –24 per group. Datasets were unbiasedly

antibody specific to tyrosine hydroxylase (TH; rabbit polyclonal; Novus Biologicals, NB 300-109; 1:500). This was followed by incubations with a biotin-conjugated anti-rabbit antibody (Vector Laboratories; 1:1000), ABC reagents (Vector Laboratories), and SigmaFast DAB Peroxidase Substrate (Sigma). These sections were then mounted on glass slides (Fisher Scientific) and allowed to dry. Sections were counterstained with Nissl (0.09% thionin for 7 min, followed by formalin acetic acid for 1 min), and glass coverslips (Fisher Scientific) were mounted using DPX mountant (Sigma). Slides were allowed to dry for at least 24 h before stereological counting.

### Stereological neuron counting

Neurons were quantified using an optical fractionator and a computer-based image analysis system. Slides were placed on a motorized stage (Ludl Electronics) attached to an Axiophot photomicroscope (Carl Zeiss Vision) containing a Hitachi HV C20 video camera. Quantification of neurons was conducted using Stereo Investigator software (MicroBrightField) as previously described (Mandir et al., 1999). In brief, staining was done on every fourth section of the mid-brain. Total number of TH-positive and Nissl-positive neurons were calculated via Stereo Investigator software for each genotype ( $n = 6-8$ ). These quantifications were multiplied by a factor of two, as only the right hemisphere of each brain was used for immunohistochemistry.

### Determination of striatal catecholamines

HPLC with electrochemical detection was performed to determine the concentration of striatal catecholamines. Snap-frozen striatal tissue from the left hemisphere of mice were weighed and sonicated in 0.2 ml of 0.1 M perchloric acid with 0.01% EDTA containing 25 g/ml 3,4-dihydroxybenzylamine (DHBA; Sigma) as an internal standard. After centrifugation ( $15,000 \times g$ , 10 min, 4°C), 20  $\mu$ l of the supernatant was injected onto a C-18 reverse phase Spheri 5, RP-18, 4.6 mm 25 cm catecholamine column (BASi). The mobile phase consisted of 0.15 M chloroacetic acid, 0.2 mM EDTA, and 0.86 mM sodium octyl sulfate, 4% acetonitrile and 2.5% tetrahydrofuran (pH 3.0). Flow rate was kept at 1.5 ml/min. Biogenic amines and their metabolites were detected by a Prostar ECD (Model 370) electrochemical detector (Varian), with the working electrode kept at 0.6 V. Data were collected and processed on a Star Chromatography Workstation 5.52 (Varian).

### Western blot analysis

Mice were perfused with ice cold  $1 \times$  PBS (Quality Biologicals, pH 7.4), and the brains were dissected from the skulls. The right hemisphere was regionally dissected on ice and immediately snap frozen. Tissue was homogenized in a  $1 \times$  RIPA Buffer (Sigma) and protease/phosphatase inhibitor cocktail (CST). Once lysed, homogenates were freeze-thawed from dry ice to ice three times. Samples were vortexed for 10–20 s at the end of each thaw. Lysates were centrifuged at 14,000 rpm (Optima TLX

←

analyzed using ROUT outlier analysis with a maximum false discovery rate (q) of 0.1%. Data were found to be normally distributed via D'Agostino and Pearson test. SDs were not found to differ significantly. Significance of means was analyzed via an ordinary one-way ANOVA ( $F_{(5,121)} = 52.80$  \*\*\*\* $p < 0.0001$ ). *Post hoc* Tukey's test was performed for and resulted in \*\*\*\* $p < 0.0001$  for wild-type versus all PolgA<sup>D257A/D257A</sup>-expressing mice and for Parkin<sup>-/-</sup> versus all PolgA<sup>D257A/D257A</sup>-expressing mice, ns, not significant. **H**, Total resting time, defined as a period of four or more seconds with no photobeam breaks, in 15-min test period. Results are the mean  $\pm$  SEM,  $n = 17-24$  per group. Datasets were unbiasedly analyzed using ROUT outlier analysis with a maximum false discovery rate (q) of 0.1%. Data were found to be normally distributed via D'Agostino and Pearson test. SDs were found to differ significantly per Brown–Forsythe test of variance. Therefore, significance of means was analyzed via a Welch one-way ANOVA ( $W(5.0,74.83) = 68.21$  \*\*\*\* $p < 0.0001$ ). *Post hoc* Dunnett's T3 test resulted in \*\*\*\* $p < 0.0001$  for wild-type versus all PolgA<sup>D257A/D257A</sup>-expressing mice and for Parkin<sup>-/-</sup> versus all PolgA<sup>D257A/D257A</sup>-expressing mice, ns, not significant. Analysis and graphs were produced using GraphPad Prism 8.4.3. Distance traveled, average speed and total resting time at three, six, and nine months is provided in Extended Data Figure 2-2. Pole test, forelimb and total strength, distance traveled, average speed, and total resting time in male and female mice at 12 months is provided in Extended Data Figure 2-3.

micro-ultracentrifuges, TLA 100.3 rotor) at 4°C for 30 min and the fractions were collected. The protein concentration was measured via BCA assay (Pierce) and analyzed via Western blot. The Novex Bis-Tris system (including 4–12% Bis-Tris gel, MOPS buffer, LDS) was used according to manufacturer's protocol; 20  $\mu$ g of protein was loaded per well. Protein was transferred to methanol-activated PVDF membranes. Membranes were stained with Ponceau to ensure even transfer. Membranes were blocked with 5% nonfat milk in  $1 \times$  PBS-T for 1 h. Membranes were washed three times for 5 min each with PBS-T. Membranes were incubated with primary antibodies in  $1 \times$  PBS-T at 4°C overnight. Antibodies used are as follows: NDUFA9 (Abcam; 1:1000), UQCRC2 (Proteintech; 1:1000), COXIV (Proteintech; 1:1000), PDHA (CST; 1:1000), SDHA (CST; 1:1000), VDAC (CST; 1:1000), LC3/II (CST; 1:1000), Parkin (CST; 1:500),  $\beta$ -actin-HRP (Thermo; 1:10,000). Thermo luminol substrates were applied according to manufacturer's protocol and membranes were imaged on a GE AI600 Chemiluminescent Imager. Western blottings were quantified using ImageJ.

### Mitochondrial enzyme activity

The activity of Complex I and IV activity in flash frozen ventral mid-brain tissue was determined by using the Complex I Enzyme Activity Microplate Assay kit (ab109721, Abcam) and the Complex IV Rodent Enzyme Activity Microplate Assay kit (ab109911, Abcam) according to the manufacturer's instructions. Briefly, tissue of ventral midbrain was dissected and homogenized with PBS, centrifuged at  $1000 \times g$  for 10 min at 4°C, and the protein concentration of collected supernatant were measured using the Bradford Assay. Detergent was added to samples after adjusting sample concentration and incubated 30 min on ice. The supernatant was collected after centrifugation at  $12,000 \times g$  for 20 min at 4°C, 250- $\mu$ g total protein per sample was resuspended in 200- $\mu$ l assay buffer, added into plate and following 3-h incubation at room temperature. Based on the oxidation reaction, colorimetric changes were recorded at 450 nm (Complex I) or 550 nm (Complex IV). The complex activity was calculated from the change in absorbance using the extinction coefficients of the respective dyes.

### mtDNA copy number

Total DNA was extracted from snap-frozen striatal tissue using Qiagen DNeasy kit. Aliquots of DNA were used for Real Time Quantitative PCR (Vii7, Applied Biosystems ABI Prism 7700 Sequence Detection System, Applied Biosystems). PowerUP SYBR green reagent (Thermo) was used per manufacturer's instructions, with 10 ng of template DNA used for amplification. The primer sequences used are as follows: mtCOXI\_6530F, 5'-AGGCTTCACCCCTAGATGACACA-3'; mtCOXI\_6647R, 5'-GTAGCGTCGTGGTATTCTCTGAA-3'; mtCOXI\_6620\_F, 5'-AGGCTTCACCCCTAGATGACACA-3'; mtCOX\_L\_6647\_R, 5'-GTAGCGTCGTGGTATTCTCTGAA-3'; mtND4\_F, 5'-AACGGATCCACAGCCGTA-3'; mtND4\_R, 5'-AGTCCTCGGGCCATGATT-3'; mtdloop\_F, 5'-TCCTCCGTGAAACC AACAA-3'; mtdloop\_R, 5'-AGCGAGAAGAGGGGCATT-3'; mtCYTB\_F, 5'-ATTCTTCATGTCGGACGAG-3'; mtCYTB\_R, 5'-TGAGCGTAGAA TGGCGTATG-3'; GAPDH\_6530\_F, 5'-GCAGTGGCAAAGTGGAGATT-3'; GAPDH\_6530\_R, 5'-GAATTTGCCGTGAGTGGAGT-3'; GAPDH\_6620\_F, 5'-GCAGTGGCAAAGTGGAGATT-3'; GAPDH\_6620\_R, 5'-GAATTTGCCGTGAGTGGAGT-3'.

Sequences of primers used to measure mtDNA copy number; mtCOXI\_6530F, mtCOXI\_6647R, GAPDH\_6530\_F, and GAPDH\_6530\_R were previously reported in (Pickrell et al., 2015); mtCOXI\_6620F, mtCOXI\_6836R, mtCYTB\_F, mtCYTB\_R, GAPDH\_6620\_F, and GAPDH\_6620\_R were previously reported previously (Stevens et al., 2015).

### Experimental design and statistical analysis

Power analysis was conducted using G\*Power3.1.9.6. Raw data supplied by the first author from Figure 1B of the original Pickrell et al., 2015 article was used to determine the appropriate effect size (Pickrell et al., 2015). To be conservative, the maximum standard deviation between groups was used (2167.146). The effect size was determined to be 0.8557729. Using this effect size, an a priori power analysis was

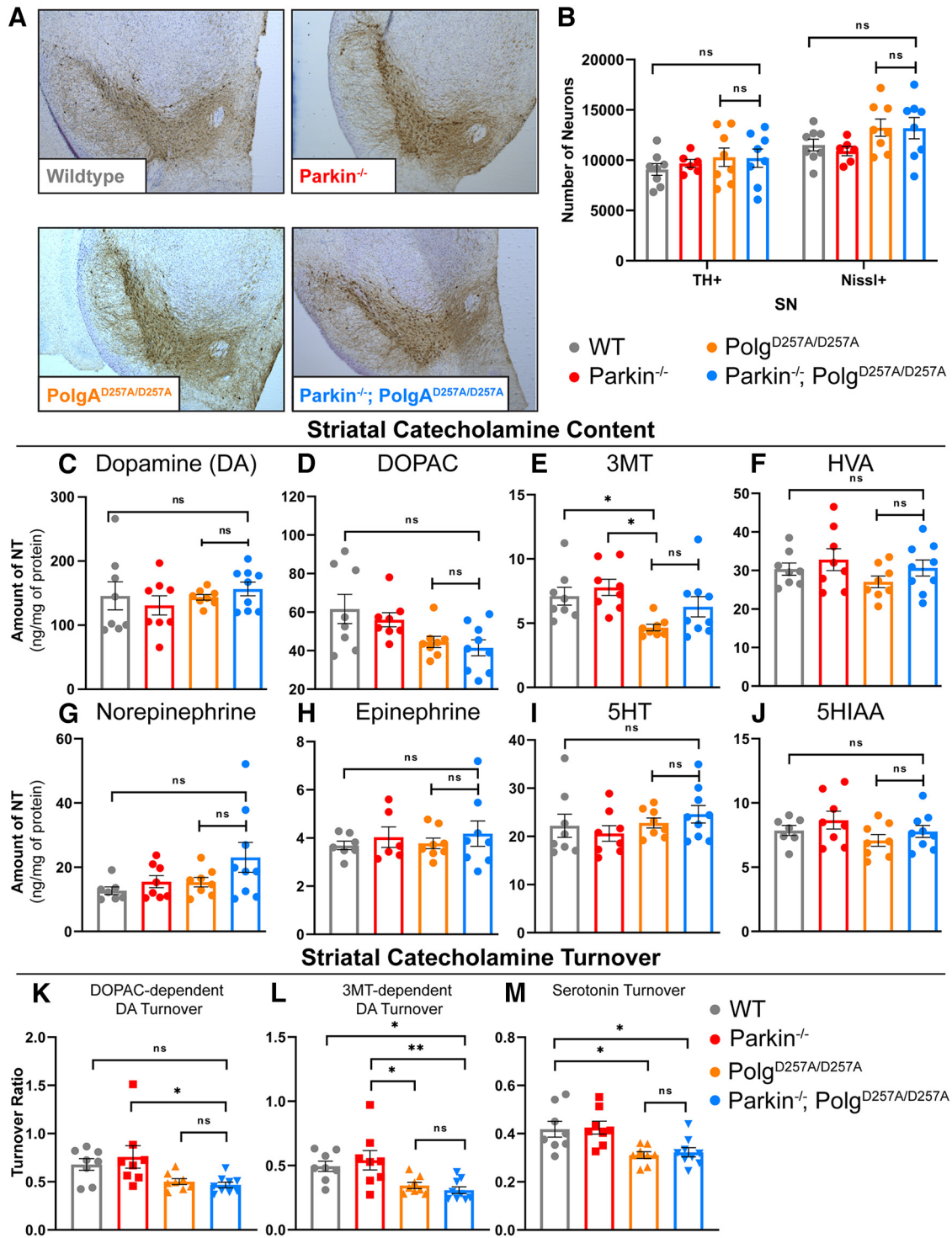


**Figure 3.** Neuropathological analysis of ventral midbrain tissue of 12-month-old mice. **A**, Representative images of immunohistochemical analysis of 12-month-old ventral midbrain sections. TH+ neurons are stained via 3'-diaminobenzidine (D)AB (Brown) and Nissl+ (a pan-neuronal marker) are stained blue. **B**, Stereological quantification of TH+ and Nissl+ neurons in the substantia nigra. Quantifications multiplied by factor of two to extrapolate to whole-brain values. Results are the mean  $\pm$  SEM,  $n = 6-8$  per group. Datasets were unbiasedly analyzed using ROUT outlier analysis with a maximum false discovery rate ( $q$ ) of 0.1%. No outliers were removed. Data were found to be normally distributed via D'Agostino and Pearson test. Data analyzed using two-way ANOVA ( $F_{(3,52)} = 2.143$ ,  $p = 0.1060$ ), ns, not significant. **C, D**, HPLC analysis of striatal dopamine and DOPAC content normalized to total protein concentration. Striatum of right hemisphere of 12-month-old mice were used. Quantifications multiplied by factor of two to extrapolate to whole-brain values. Results are the mean  $\pm$  SEM,  $n = 8-9$  per group. Datasets were unbiasedly analyzed using ROUT outlier analysis with a maximum false discovery rate ( $q$ ) of 0.1%. Data were found to be normally distributed via D'Agostino and Pearson test. SDs were found to differ significantly per Brown-Forsythe test of variance. Therefore, significance of means was analyzed via a Welch one-way ANOVA (**D**:  $W(3.0, 13.86) = 0.6434$ ,  $p = 0.5999$ ; **E**:  $W(3.0, 15.59) = 3.661$ ,  $*p = 0.0357$ ). *Post hoc* Dunnett's T3 test resulted in no significant differences between groups, ns, not significant. **E**, HPLC analysis of striatal 3MT content normalized to total protein concentration. Striatum of right hemisphere of 12-month-old mice were used. Quantifications multiplied by factor of two to extrapolate to whole-brain values. Results are the median  $\pm$  SEM,  $n = 8-9$  per group. Datasets were unbiasedly analyzed using ROUT outlier analysis with a maximum false discovery rate ( $q$ ) of 0.1%. Data were found to be non-normally distributed per D'Agostino and Pearson test. Significance of medians was analyzed via Kruskal-Wallis nonparametric ANOVA (KW(4,33) = 13.17,  $*p = 0.0043$ ). *Post hoc* Kruskal-Wallis test for multiple comparisons resulted in  $**p = 0.0024$  for wild-type versus PolgA<sup>D257A/D257A</sup> and  $**p = 0.0042$  for Parkin<sup>-/-</sup> versus PolgA<sup>D257A/D257A</sup>, ns, not significant. **F-H**, HPLC analysis of striatal HVA, norepinephrine, and epinephrine content normalized

performed. Power was maintained at 80% and the resulting total sample size was determined to be 20 ( $n = 5/\text{group}$ ).

The remaining statistical analyses were conducted using GraphPad Prism version 8.4.3 and 9.4.1 software. ROUT analysis for outlier identification with a max false discovery rate at 0.1% was performed on each dataset. Next, the D'Agostino and Pearson test for normality was conducted. If data were distributed normally, the Brown–Forsythe test of variance was performed to determine whether SDs differed significantly between groups. If SDs did not differ, one-way or two-way ANOVA followed by Tukey's analyses was performed to determine the significance of differences among multiple experimental groups. If SDs significantly differed, significance of means was analyzed via Welch one-way ANOVA followed by *post hoc* Dunnett's T3 test of multiple comparisons. Data are expressed as the mean  $\pm$  SEM, and values with  $p < 0.05$  considered statistically significant. If data were not normally distributed ( $\geq 50\%$  of the groups were non-normally distributed), significance of medians was analyzed via Kruskal–Wallis test followed by *post hoc* Kruskal–Wallis test of multiple comparisons. Data in these analyses are expressed as the median  $\pm$  SEM, and values with  $p < 0.05$  considered statistically significant.

## Results

We generated  $\text{Parkin}^{-/-}/\text{PolgA}^{\text{D257A/D257A}}$  and appropriate littermate controls via the cross shown in Figure 1A. Because female mice are the primary contributor of mitochondria to pups and  $\text{PolgA}^{\text{D257A/+}}$  parents may still accumulate damaged mitochondria over time, we used  $\text{PolgA}^{\text{D257A/+}}$  male mice at every possible step in the breeding scheme, thus limiting the potential vertical transfer of  $\text{PolgA}^{\text{D257A/+}}$ -dependent mtDNA mutations to newborn mice. Mice were born at expected Mendelian ratios and appeared normal. Genotypes were confirmed via PCR and gel electrophoresis (Fig. 1B). Both male and female mice harboring the  $\text{PolgA}^{\text{D257A/D257A}}$  exhibited reduced body weight by 12 months (Fig. 1C,D). Previous reports stated that loss of Parkin partially rescued the splenomegaly phenotype observed in the  $\text{PolgA}^{\text{D257A/D257A}}$  line (Pickrell et al., 2015). We did not observe worsening or amelioration of

←

to total protein concentration. Striatum of right hemisphere of 12-month-old mice were used. Quantifications multiplied by factor of two to extrapolate to whole-brain values. Results are the median  $\pm$  SEM,  $n = 8–9$  per group. Datasets were unbiasedly analyzed using ROUT outlier analysis with a maximum false discovery rate ( $q$ ) of 0.1%. Data were found to be normally distributed via D'Agostino and Pearson test. SDs were not found to differ significantly. Significance of means was analyzed via an ordinary one-way ANOVA (**G**:  $F_{(3,29)} = 1.2$   $p = 0.3050$ ; **H**:  $F_{(3,28)} = 2.4$   $p = 0.0868$ ; **H**:  $F_{(2,25)} = 0.3$   $p = 0.7653$ ), ns, not significant. **I, J**, HPLC analysis of striatal 5HT and 5HIAA, a 5HT metabolite, content normalized to total protein concentration. Striatum of right hemisphere of 12-month-old mice were used. Quantifications multiplied by factor of two to extrapolate to whole-brain values. Results are the median  $\pm$  SEM,  $n = 8–9$  per group. Datasets were unbiasedly analyzed using ROUT outlier analysis with a maximum false discovery rate ( $q$ ) of 0.1%. Data were found to be normally distributed via D'Agostino and Pearson test. SDs were not found to differ significantly. Significance of means was analyzed via an ordinary one-way ANOVA (**J**:  $F_{(3,29)} = 0.8779$   $p = 0.4642$ ; **K**:  $F_{(3,28)} = 1.529$   $p = 0.2286$ ), ns, not significant. **K**, DOPAC-dependent dopamine turnover as assessed by (DOPAC+HVA)/dopamine. Significance of means analyzed via ordinary one-way ANOVA ( $F_{(2,29)} = 4.367$   $*p = 0.0118$ ). *Post hoc* Tukey's test resulted in  $*p = 0.0208$  for  $\text{Parkin}^{-/-}$  versus  $\text{Parkin}^{-/-}/\text{PolgA}^{\text{D257A/D257A}}$ , ns, not significant. **L**, 3MT-dependent dopamine turnover as assessed by (3MT+HVA)/dopamine. Significance of means analyzed via ordinary one-way ANOVA ( $F_{(2,29)} = 6.282$   $**p = 0.0020$ ). *Post hoc* Tukey's test resulted in  $*p = 0.0310$  for wild-type versus  $\text{Parkin}^{-/-}/\text{PolgA}^{\text{D257A/D257A}}$ ,  $*p = 0.0254$  for  $\text{Parkin}^{-/-}$  versus  $\text{PolgA}^{\text{D257A/D257A}}$ , and  $**p = 0.0049$  for  $\text{Parkin}^{-/-}$  versus  $\text{Parkin}^{-/-}/\text{PolgA}^{\text{D257A/D257A}}$ , ns, not significant. **M**, Serotonin (5HT) turnover as assessed by 5HIAA/5HT. Significance of means analyzed via ordinary one-way ANOVA ( $F_{(2,29)} = 6.449$   $**p = 0.0118$ ). *Post hoc* Tukey's test resulted in  $*p = 0.0195$  for wild-type versus  $\text{PolgA}^{\text{D257A/D257A}}$ ,  $*p = 0.0355$  for wild-type versus  $\text{Parkin}^{-/-}/\text{PolgA}^{\text{D257A/D257A}}$ ,  $*p = 0.0121$  for  $\text{Parkin}^{-/-}$  versus  $\text{PolgA}^{\text{D257A/D257A}}$ , and  $**p = 0.0222$  for  $\text{Parkin}^{-/-}$  versus  $\text{Parkin}^{-/-}/\text{PolgA}^{\text{D257A/D257A}}$ , ns, not significant. Analysis and graphs were produced using GraphPad Prism 8.4.3.

hepatosplenomegaly or cardiac hypertrophy in  $\text{Parkin}^{-/-}/\text{PolgA}^{\text{D257A/D257A}}$  mice compared with  $\text{PolgA}^{\text{D257A/D257A}}$  mice (Fig. 1E–G).

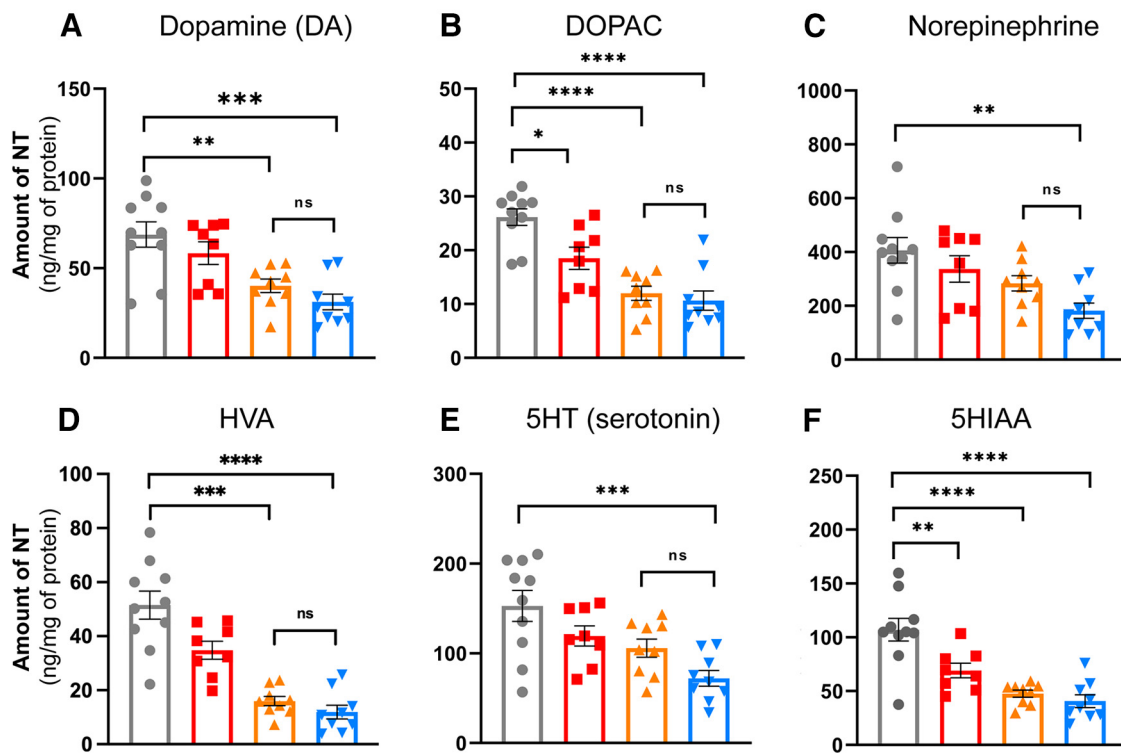
## Absence of nigro-striatal-dependent motor dysfunction in $\text{Parkin}^{-/-}/\text{PolgA}^{\text{D257A/D257A}}$ mice

We first tested whether  $\text{Parkin}^{-/-}/\text{PolgA}^{\text{D257A/D257A}}$  mice displayed progressive motor dysfunction or behavioral deficits. Mice were subjected to Openfield and grip strength analysis every three months until 12 months of age and pole tests at 12 months of age, the time point at which broad respiratory chain dysfunction in  $\text{PolgA}^{\text{D257A/D257A}}$  has been reported (Ross et al., 2013). The pole test is a widely used behavioral test for PD-related nigral-striatal-dependent motor dysfunction in PD mouse models (Ogawa et al., 1985). The pole test is defined by placing a mouse face up on top of a pole of a prespecified height and recording the time it takes the mouse to turn around and successfully run down the pole (Matsuura et al., 1997; Fig. 2A). We observed no significant difference in latency times for the pole test for 12-month-old  $\text{Parkin}^{-/-}/\text{PolgA}^{\text{D257A/D257A}}$  mice compared with wild-type (Fig. 2B).

Neuromuscular strength was analyzed via grip force readings of both forelimbs and total limbs (Fig. 2C). We observed significant reductions in total limb strength in all  $\text{PolgA}^{\text{D257A/D257A}}$ -expressing lines compared with wild type at 12 months (Fig. 2D) as well as a reduction in forelimb strength between 12-month-old wild-type and  $\text{Parkin}^{-/-}/\text{PolgA}^{\text{D257A/D257A}}$  cohorts (Fig. 2E). Differences in forelimb strength were first seen in both  $\text{PolgA}^{\text{D257A/D257A}}$  and  $\text{Parkin}^{-/-}/\text{PolgA}^{\text{D257A/D257A}}$  cohorts at six months (Extended Data Fig. 2-1A–C). However, these differences in forelimb strength were not present at nine months (Extended Data Fig. 2-2A–C). Furthermore, reductions in total limb strength were observed in  $\text{Parkin}^{-/-}/\text{PolgA}^{\text{D257A/D257A}}$  mice at six and nine months (Extended Data Fig. 2-1D–F). It should be noted that there were no differences between any  $\text{PolgA}^{\text{D257A/D257A}}$ -expressing groups at 12 months, confirming that neuromuscular strength deficits at 12 months are ultimately a result of the  $\text{PolgA}^{\text{D257A/D257A}}$  mutation (Fig. 2D,E). Unexpectedly,  $\text{Parkin}^{-/-}$  mice displayed reductions in total limb strength at nearly all time points. Because  $\text{Parkin}^{-/-}$  mice were observed to weigh slightly more than wild-type mice at nearly every time point, we believe that normalization to body weight contributed to some of the differences observed in the grip strengths. These findings are supported by analysis of non-normalized force readings, which demonstrated no differences between groups at early time points, with significant reductions in both forelimb and total limb strength in all  $\text{PolgA}^{\text{D257A/D257A}}$ -expressing lines compared with wild-type and  $\text{Parkin}^{-/-}$  at 12 months.

Locomotor activity was investigated using the Openfield test, a behavioral test commonly performed to assess locomotion, exploration, and emotionality in rodents. There was a progressive decline in the distance traveled in all cohorts with the  $\text{PolgA}^{\text{D257A/D257A}}$  mutation when compared with wild-type and  $\text{Parkin}^{-/-}$  mice at 12 months (Fig. 2F). This paralleled a previous report of reduced locomotor activity in aged  $\text{PolgA}^{\text{D257A/D257A}}$  mice (Dai et al., 2013). All mice with the  $\text{PolgA}^{\text{D257A/D257A}}$  background exhibited significant reductions in the average speed of locomotion at 12 months (Fig. 2G). Furthermore, they displayed an increase in resting time, quantified as a period of four or more seconds without movement, by 12 months (Fig. 2H). These changes were initially seen at six months, with both  $\text{PolgA}^{\text{D257A/D257A}}$  and  $\text{Parkin}^{-/-}/\text{PolgA}^{\text{D257A/D257A}}$  mice demonstrating loss of speed and distance compared with controls (Extended Data Fig. 2-2B,E).

## Olfactory Bulb Catecholamine Content



## Olfactory Bulb Catecholamine Turnover

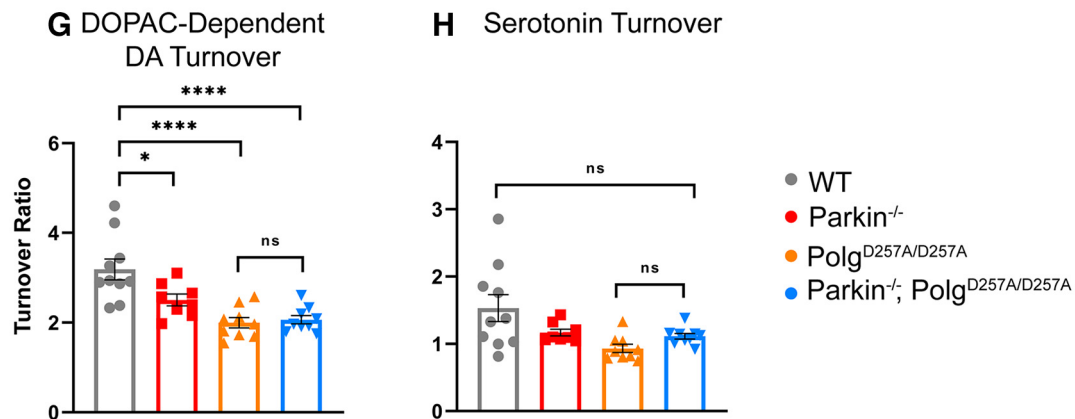


**Figure 4.** Neuropathological analysis of striatal tissue of 12-month-old mice. **A–C**, HPLC analysis of olfactory bulb dopamine, DOPAC, and norepinephrine content normalized to total protein concentration. Olfactory bulb of right hemisphere of 12-month-old mice were used. Quantifications multiplied by factor of two to extrapolate to whole-brain values. Results are the mean  $\pm$  SEM,  $n = 8–9$  per group. Datasets were unbiasedly analyzed using ROUT outlier analysis with a maximum false discovery rate ( $q$ ) of 0.1%. Data were found to be normally distributed via D’Agostino and Pearson test. SDs were not found to differ significantly. Significance of means was analyzed via an ordinary one-way ANOVA (**A**:  $F_{(3,32)} = 9.4$  \*\*\*\* $p = 0.0001$ ; **B**:  $F_{(3,32)} = 2.4$  \*\*\*\* $p < 0.00001$ ; **C**:  $F_{(3,32)} = 5.886$  \*\* $p = 0.0026$ ). *Post hoc* Tukey’s test resulted in **A**: \*\* $p = 0.046$  for wild-type versus Parkin<sup>-/-</sup>/Polg<sup>D257A/D257A</sup>, \*\*\* $p = 0.0002$  for wild-type versus Parkin<sup>-/-</sup>/Polg<sup>D257A/D257A</sup>, and \* $p = 0.0116$  for Parkin<sup>-/-</sup> versus Parkin<sup>-/-</sup>/Polg<sup>D257A/D257A</sup>; **B**: \* $p = 0.0154$  for wild-type versus Parkin<sup>-/-</sup>, \*\*\*\* $p < 0.00001$  for wild-type versus Polg<sup>D257A/D257A</sup> and for wild-type versus Parkin<sup>-/-</sup>/Polg<sup>D257A/D257A</sup>, and \* $p = 0.0153$  for Parkin<sup>-/-</sup> versus Parkin<sup>-/-</sup>/Polg<sup>D257A/D257A</sup>; **C**: \*\* $p = 0.0015$  for wild-type versus Parkin<sup>-/-</sup>/Polg<sup>D257A/D257A</sup>, ns, not significant. **D**, HPLC analysis of olfactory bulb HVA content normalized to total protein concentration. Olfactory bulb of right hemisphere of 12-month-old mice were used. Quantifications multiplied by factor of two to extrapolate to whole-brain values. Results are the mean  $\pm$  SEM,  $n = 8–9$  per group. Datasets were unbiasedly analyzed using ROUT outlier analysis with a maximum false discovery rate ( $q$ ) of 0.1%. Data were found to be normally distributed via D’Agostino and Pearson test. SDs were found to differ significantly per Brown–Forsythe test of variance. Therefore, significance of means was analyzed via a Welch one-way ANOVA (**D**:  $W(3.0,16.71) = 28.77$  \*\*\*\* $p < 0.00001$ ). *Post hoc* Dunnett’s T3 test resulted in \*\*\*\* $p = 0.046$  for wild-type versus Polg<sup>D257A/D257A</sup>, \*\*\*\* $p < 0.00001$  for wild-type versus Parkin<sup>-/-</sup>/Polg<sup>D257A/D257A</sup>, \*\* $p = 0.0031$  for Parkin<sup>-/-</sup> versus Polg<sup>D257A/D257A</sup>, and \*\*\*\* $p = 0.0007$  for Parkin<sup>-/-</sup> versus Parkin<sup>-/-</sup>/Polg<sup>D257A/D257A</sup>, ns, not significant. **E, F**, HPLC analysis of olfactory bulb 5HT and 5HIAA content normalized to total protein concentration. Olfactory bulb of right hemisphere of 12-month-old mice were used. Quantifications multiplied by factor of two to extrapolate to whole-brain values. Results are the mean  $\pm$  SEM,  $n = 8–9$  per group. Datasets were unbiasedly analyzed using ROUT outlier analysis with a maximum false discovery rate ( $q$ ) of 0.1%. Data were found to be normally distributed via D’Agostino and Pearson test. SDs were not found to differ significantly. Significance of means was analyzed via an ordinary one-way ANOVA (**E**:  $F_{(3,32)} = 7.249$  \*\*\*\* $p = 0.0008$ ; **F**:  $F_{(3,32)} = 17.31$  \*\*\*\* $p < 0.00001$ ). *Post hoc* Tukey’s test resulted in **E**: \*\*\*\* $p = 0.004$  for wild-type versus Parkin<sup>-/-</sup>/Polg<sup>D257A/D257A</sup>,

These reductions progressed in significance and severity from six to nine months (Extended Data Fig. 2-2C,F). Similarly, an increase in resting time was observed in *Parkin*<sup>-/-</sup>/*PolgA*<sup>D257A/D257A</sup> at six months, and by nine months both *PolgA*<sup>D257A/D257A</sup> and *Parkin*<sup>-/-</sup>/*PolgA*<sup>D257A/D257A</sup> mice demonstrated significant increases in their time spent resting (Extended Data Fig. 2-2H,I). The loss of endogenous Parkin in the context of *PolgA*<sup>D257A/D257A</sup> did not significantly impact the neuromuscular behavioral defects observed. Furthermore, no sex effects were observed in behavior tests (Extended Data Fig. 2-3).

### Dopaminergic neurons in the SNpc remain intact in *Parkin*<sup>-/-</sup>/*PolgA*<sup>D257A/D257A</sup> mice

Thus far, our data has suggested that behavioral changes were the result of the *PolgA*<sup>D257A/D257A</sup> genotype. To further explore any underlying neurochemical deficits in *Parkin*<sup>-/-</sup>/*PolgA*<sup>D257A/D257A</sup>, we performed immunohistochemistry for TH<sup>+</sup> neurons in ventral midbrain tissue of 12-month-old mice (Fig. 3A). Unbiased stereologic cell counting revealed no observable changes in the amount of TH<sup>+</sup> or Nissl<sup>+</sup> neurons in the SNpc of any of the groups, including *Parkin*<sup>-/-</sup>/*PolgA*<sup>D257A/D257A</sup> mice (Fig. 3B). These data indicate that there was no dopaminergic neurodegeneration in the ventral midbrain.

We next assessed striatal dopamine and dopamine degradation products in 12-month-old mice. In agreement with our stereological data, there were no significant changes in dopamine or its degradation products dihydroxyphenylacetic acid (DOPAC), homovanillic acid (HVA), norepinephrine, or epinephrine (Fig. 3C,D,F-H). Similar to prior reports (Pickrell et al., 2015), we did observe a reduction in 3-methoxytyramine (3-MT), a dopamine degradation product, in *PolgA*<sup>D257A/D257A</sup> mice compared with both wild-type and *Parkin*<sup>-/-</sup> mice; however, we saw no reduction in *Parkin*<sup>-/-</sup>/*PolgA*<sup>D257A/D257A</sup> mice (Fig. 3E).

Another method to assess striatal catecholamine dysregulation is to calculate turnover rates. Dopamine turnover can be determined by using the following equations: (1) DOPAC-dependent dopamine turnover [(DOPAC + HVA)/dopamine] or (2) 3MT dependent dopamine turnover [(3MT + HVA)/dopamine]. Using this approach, we found a significant reduction in DOPAC-dependent dopamine turnover in *Parkin*<sup>-/-</sup>/*PolgA*<sup>D257A/D257A</sup> mice compared with *Parkin*<sup>-/-</sup> mice, but not wild-type mice (Fig. 3K). Analysis of 3MT-dependent dopamine turnover showed substantial reductions in *Parkin*<sup>-/-</sup>/*PolgA*<sup>D257A/D257A</sup> mice and *PolgA*<sup>D257A/D257A</sup> mice compared with *Parkin*<sup>-/-</sup> mice (Fig. 3L). There was also a reduction in *Parkin*<sup>-/-</sup>/*PolgA*<sup>D257A/D257A</sup> mice versus wild-type mice (Fig. 3L). These results imply that both *PolgA*<sup>D257A/D257A</sup> mice and *Parkin*<sup>-/-</sup>/*PolgA*<sup>D257A/D257A</sup> mice exhibit some striatal dopamine dysregulation without dopaminergic neuronal loss. These results agree with previous findings, which report striatal

dopamine dysregulation in *PolgA*<sup>D257A/D257A</sup> mice (Dai et al., 2013). No differences were observed between *PolgA*<sup>D257A/D257A</sup> mice and *Parkin*<sup>-/-</sup>/*PolgA*<sup>D257A/D257A</sup> mice in dopamine or in dopamine turnover, suggesting that dysregulation is a result of the *PolgA*<sup>D257A/D257A</sup> knock-in and is not significantly impacted by Parkin loss.

Serotonergic neurons from the raphe nuclei project, in part, to the striatum and are critical for a variety of neurologic functions including mood, memory processing, sleep, and cognition (Charnay and Léger, 2010). Analysis of striatal serotonin, also known as 5-hydroxytryptamine (5-HT) and its degradation product 5-hydroxyindoleacetic acid (5HIAA) demonstrated no differences between cohorts at 12 months of age (Fig. 3I,J). These data are contrary to previous work which reports a significant increase in serotonin levels in striatal tissue (Pickrell et al., 2015). Serotonin turnover can be calculated by normalizing 5HIAA to 5-HT. We observed a significant reduction in serotonin turnover of *PolgA*<sup>D257A/D257A</sup> mice compared with both wild-type and *Parkin*<sup>-/-</sup> mice (Fig. 3M), implying that aged *PolgA*<sup>D257A/D257A</sup> mice experience striatal catecholamine and indolamine dysregulation.

An early clinical sign that precedes motor dysfunction in PD patients is anosmia or the loss of one's sense of smell. A prior report indicated a significant increase in serotonin and norepinephrine levels in striatal and olfactory bulb tissue of *Parkin*<sup>-/-</sup>/*PolgA*<sup>D257A/D257A</sup> mice (Pickrell et al., 2015). They postulated that the upregulation of these neurotransmitters may be a compensatory mechanism by which neurons react to the loss of dopamine. Our analysis of these brain regions, however, displayed reductions in serotonin (5-HT) in *Parkin*<sup>-/-</sup>/*PolgA*<sup>D257A/D257A</sup> mice, as well as significant decreases in 5HIAA in all mice expressing the *PolgA*<sup>D257A/D257A</sup> mutation (Fig. 4E,F). Interestingly, there were no substantial differences in serotonin turnover, implying that serotonin dysregulation in the olfactory bulb occurs as a result of reduced serotonin levels, not in the ability to breakdown serotonin (Fig. 4H). Our analysis also revealed a significant decline in dopamine, DOPAC, HVA, and DOPAC-dependent dopamine turnover in all *PolgA*<sup>D257A/D257A</sup>-expressing mice (Fig. 4A, B,D). These differences are likely because of the effect of mtDNA mutations, as both *PolgA*<sup>D257A/D257A</sup> mice and *Parkin*<sup>-/-</sup>/*PolgA*<sup>D257A/D257A</sup> were affected and loss of Parkin did not lead to further decline in metabolite concentrations. Contrary to a prior report (Pickrell et al., 2015), we observed a reduction in olfactory bulb norepinephrine in *Parkin*<sup>-/-</sup>/*PolgA*<sup>D257A/D257A</sup> mice (Fig. 4C). *Parkin*<sup>-/-</sup> mice also displayed reductions in dopamine metabolites, suggesting that germline *Parkin*<sup>-/-</sup> mice themselves exhibit olfactory-bulb dopamine dysregulation at 12 months of age (Fig. 4B,G). This was expected as reductions in olfactory bulb dopamine were reported in this specific germline *Parkin*<sup>-/-</sup> line (Von Coelln et al., 2004).

### Loss of parkin does not enhance mitochondrial dysfunction in *PolgA*<sup>D257A/D257A</sup> mice

To further investigate whether loss of endogenous Parkin affects mitochondrial dysfunction induced by the *PolgA*<sup>D257A/D257A</sup> mutation, we quantified the steady-state expression level of mitochondrial markers in the ventral midbrain of 12-month-old mice. Western blots were performed with a panel of commercially available antibodies. We found no differences in expression levels of most mitochondrial markers tested, including NDUFA9 (subunit of Complex I) and UQCRC2 (subunit of Complex III);

F: \*\**p* = 0.0056 for wild-type versus *Parkin*<sup>-/-</sup>, \*\*\*\**p* < 0.00001 for wild-type versus *PolgA*<sup>D257A/D257A</sup> and for wild-type versus *Parkin*<sup>-/-</sup>/*PolgA*<sup>D257A/D257A</sup>, ns, not significant. G, DOPAC-dependent dopamine turnover as assessed by (DOPAC + HVA)/dopamine. Significance of means analyzed via ordinary one-way ANOVA ( $F_{(3,32)} = 12.41$ , \*\*\*\**p* < 0.00001). *Post hoc* Tukey's test resulted in \**p* = 0.0260 for wild-type versus *Parkin*<sup>-/-</sup>, \*\*\*\**p* < 0.00001 for wild-type versus *PolgA*<sup>D257A/D257A</sup> and for wild-type versus *Parkin*<sup>-/-</sup>/*PolgA*<sup>D257A/D257A</sup>, ns, not significant. H, Serotonin (5HT) turnover as assessed by 5HIAA/5HT. Data were found to be normally distributed via D'Agostino and Pearson test. SDs were found to differ significantly per Brown-Forsythe test of variance. Therefore, significance of means was analyzed via a Welch one-way ANOVA ( $D: W(3.0,17.32) = 4.339$ , \**p* = 0.0142). *Post hoc* Dunnett's T3 test resulted in no significant differences (ns) between groups. Analysis and graphs were produced using GraphPad Prism 8.4.3.



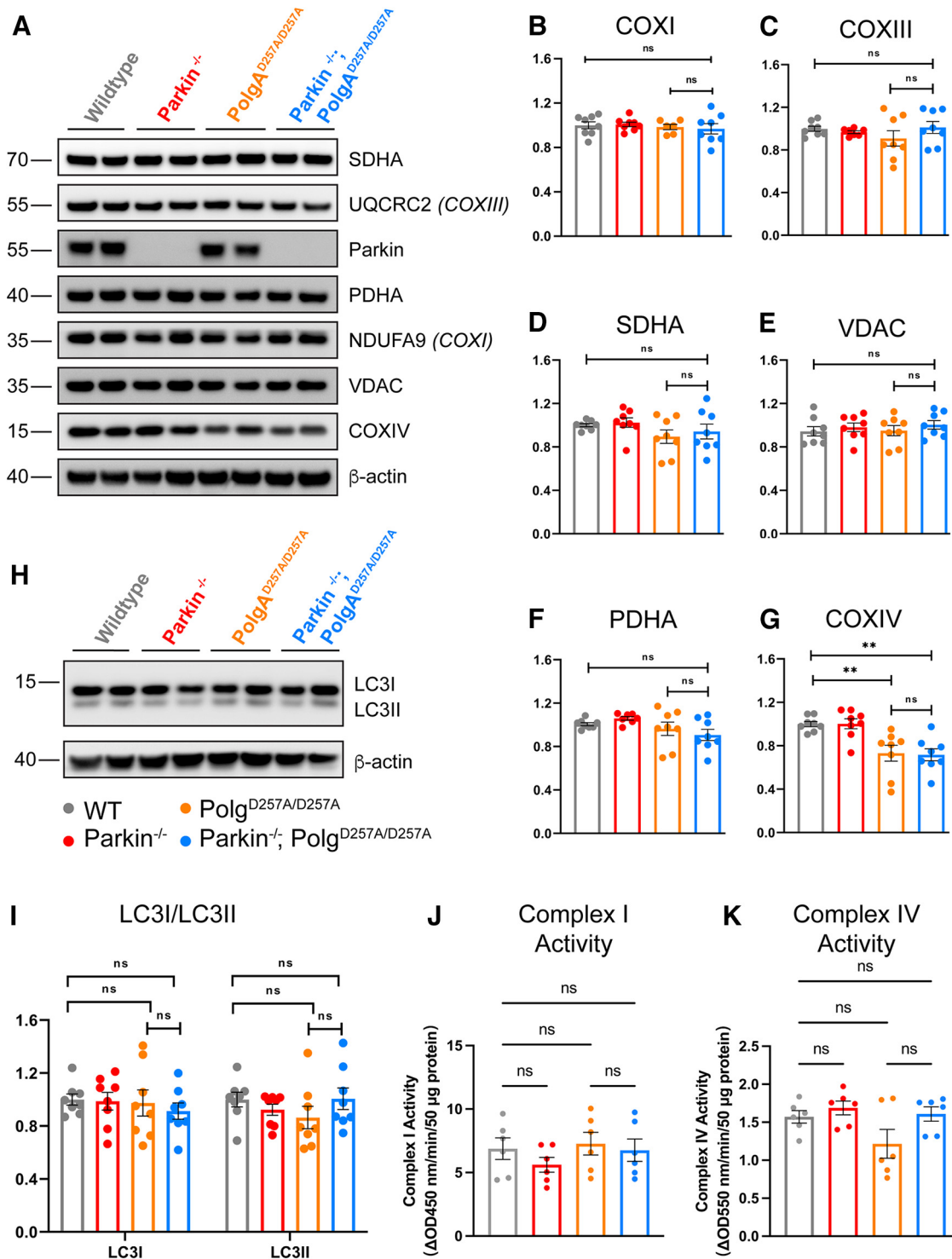


**Figure 5.** Steady-state expression of mitochondrial and mitophagy markers. **A**, Representative Western blot illustrating mitochondrial marker expression in ventral midbrain tissue of 12-month-old mice. **B–E**, Quantification of Western blot mitochondrial marker expression analysis of ventral midbrain tissue of 12-month-old mice. Results are the mean  $\pm$  SEM,  $n = 8$  mice per group. Experiments were run in a minimum of experimental triplicate with the average of results used for analysis. ImageJ was used for optical density analysis. Quantifications were normalized to  $\beta$ -actin to account for loading differences and then to wild-type values to normalize against batch effect. Datasets were unbiasedly analyzed using ROUT outlier analysis with a maximum false discovery rate ( $q$ ) of 0.1%. Data were found to be normally distributed via D’Agostino and Pearson test. SDs were found to differ significantly per Brown–Forsythe test, likely because of batch effect. Therefore, significance of means was analyzed via a Welch one-way ANOVA (**B**:  $W(3,0,13.89) = 0.2700$   $p = 0.8459$ ; **C**:  $W(3,13.58) = 0.7985$   $p = 0.5156$ ; **D**:  $W(3,13.98) = 3.607$   $*p = 0.0406$ ; **E**:  $W(3,13.0) = 1.145$   $p = 0.3068$ ). *Post hoc* Dunnett’s T3 multiple comparisons test was conducted on **D** data and resulted in no significant (ns) differences between groups. **F, G**, Quantification of Western blot mitochondrial marker expression analysis of ventral midbrain tissue of 12-month-old mice. Results are the mean  $\pm$  SEM,  $n = 8$  per group. Experiments were run in a minimum of experimental triplicate with the average of results used for analysis. ImageJ was used for optical density analysis. Quantifications were normalized to  $\beta$ -actin to account for loading differences and then to wild-type values to normalize against batch effect. Datasets were unbiasedly analyzed using ROUT outlier analysis with a maximum false discovery rate ( $q$ ) of 0.1%. Data were found to be normally distributed via D’Agostino and Pearson test. SDs were not found to differ significantly per Brown–Forsythe test. Significance of means was analyzed via ordinary one-way ANOVA (**F**:  $F_{(3,28)} = 9.173$   $***p = 0.0002$ ; **G**:  $F_{(3,28)} = 0.4631$   $p = 0.9739$ ). *Post hoc* Tukey’s test for data in **F** resulted in  $**p = 0.0064$  for wild-type versus PolgA<sup>D257A/D257A</sup>,  $**p = 0.0039$  for wild-type versus Parkin<sup>-/-</sup>/PolgA<sup>D257A/D257A</sup>,  $**p = 0.0059$  for Parkin<sup>-/-</sup> versus PolgA<sup>D257A/D257A</sup>, and  $**p = 0.0036$  for Parkin<sup>-/-</sup> versus

Fig. 5B–F; Extended Data Fig. 5-1A,B). There were, however, significant reductions in the levels of Complex IV (Fig. 5G; Extended Data Fig. 5-1A,B). This is understandable as NDUFA9, UQCRC2, succinate dehydrogenase (SDHA) complex flavo-protein subunit A (a subunit of Complex II), pyruvate dehydrogenase E1 subunit  $\alpha$  1, and voltage-dependent anion-selective channel 1 (VDAC1) are nuclear-encoded mitochondrially-targeted proteins, whereas COX4I1 (a subunit of Complex IV) is a mitochondrially-encoded subunit and would be directly affected by mtDNA mutations.

We further assessed whether loss of endogenous Parkin impacted mitochondrial complex activity in flash-frozen ventral midbrain tissue of 12-month-old mice. We observed no differences in Complex I or Complex IV activities comparing wild-type to Polg<sup>D257A/D257A</sup> and Parkin<sup>-/-</sup>; Polg<sup>D257A/D257A</sup> (Fig. 5J,K). In addition, there were no changes in the levels of the parkin substrates AIMP2 or NLRP3 implicated in the death of DA neurons (Y. Lee et al., 2013; Panicker et al., 2022) in adult Parkin<sup>-/-</sup> mice (Extended Data Fig. 5-2A–D).

Because Parkin is known to be a key player in mitophagy, we investigated whether loss of Parkin effected expression levels of mitophagy markers. The conversion of soluble LC3I to activated, lipid-conjugated LC3II is considered to be necessary for autophagosome formation, a required step for mitophagy (Stevens et al., 2015). Therefore, we analyzed the steady-state levels of LC3I and LC3II as a readout for active mitophagy (Tanida et al., 2008; Stevens et al., 2015). We observed no significant differences between cohorts in LC3I or LC3II, suggesting

that Parkin<sup>-/-</sup>/PolgA<sup>D257A/D257A</sup> mice maintain the ability to form autophagosomes (Fig. 5H,I).

Assessing mtDNA copy number is an indirect readout of the number of mitochondria per cell in a given amount of tissue (Malik and Czajka, 2013). It can also be used to investigate deficits in mitophagy, which would lead to an accumulation of damaged mitochondria and mtDNA, or mitochondrial biogenesis, which would result in a reduction of the mitochondrial pool and mtDNA. Because the depletion of mtDNA in whole-brain lysates of PolgA<sup>D257A/D257A</sup> mice was previously reported (Pickrell et al., 2015), suggesting defunct mitochondrial biogenesis, we next determined the mtDNA copy number in striatal tissue of 12-month-old mice (Stevens et al., 2015). This technique is done by isolating total DNA from tissue and performing qRT-PCR using mtDNA-specific primers (Fig. 6A; Materials and Methods). These results are then normalized to a nuclear encoded house-keeping gene, such as GAPDH, to to normalize the variance between samples, and then again to wild-type values to normalize against batch effect. We ran a panel of mtDNA primers probing several different loci, including ND4, COXI, CYTB, and the Dloop region (Pickrell et al., 2015; Stevens et al., 2015; Fig. 6G). During our initial analysis we used a mixed effects model with matching across rows, which assumes that all loci analyzed depend on the expression level of each other, appropriate in the case of mtDNA as the mitochondrial genome is circular dsDNA (Fig. 6C). This mixed-effects model also accounts for nonindependence between samples, meaning it accounts for the same biological samples being tested at each locus. When employing this statistical method, we observed no significant differences in the copy number of most mtDNA loci, indicating that mtDNA copy number remains unchanged in ventral midbrain tissue of PolgA<sup>D257A/D257A</sup> mice, regardless of the absence or presence of Parkin (Fig. 6G). Interestingly, the mixed-effects model found a consistent and substantial increase in the copy number of the Dloop region, the highly conserved origin of replication of mtDNA, in PolgA<sup>D257A/D257A</sup> mice and Parkin<sup>-/-</sup>/PolgA<sup>D257A/D257A</sup> mice.

Because of the above results, we further analyzed each mtDNA loci individually via one-way ANOVAs as previously described (Pickrell et al., 2015). We found these results to be loci-dependent. Both primer sets to COXI exhibited significant reductions in mtDNA copy number in PolgA<sup>D257A/D257A</sup> mice and Parkin<sup>-/-</sup>/PolgA<sup>D257A/D257A</sup> mice, implying decreased mitochondrial mass in these cohorts (Fig. 6B,C). Although the level of statistical significance varied between COXI primer sets, these results are similar to mtDNA copy number analysis previously reported (Pickrell et al., 2015). Contrarily, there appeared to be no differences between mouse cohorts using primers specific to CYTB (Fig. 6D). There was a substantial decrease in the amplification of ND4 in PolgA<sup>D257A/D257A</sup> mice, but not Parkin<sup>-/-</sup>/PolgA<sup>D257A/D257A</sup> mice (Fig. 6E). Moreover, one-way ANOVA analysis further confirmed the increase in Dloop copy number in PolgA<sup>D257A/D257A</sup> mice and Parkin<sup>-/-</sup>/PolgA<sup>D257A/D257A</sup> mice (Fig. 6F). It should be noted that loss of Parkin did not lead to further reductions in mtDNA copy number, regardless of the gene loci tested. Taken together, these results suggest that quantifying mtDNA copy number via mtDNA amplification may not be a sufficient method to investigate mitochondrial mass in mouse lines that accumulate mtDNA mutations.

## Discussion

In this study, we originally set out to expand on previous work which reported dopaminergic neurodegeneration and corresponding

←  
 Parkin<sup>-/-</sup>/PolgA<sup>D257A/D257A</sup>, ns, not significant. **H**, Representative Western blot illustrating blot mitophagy marker expression analysis in ventral midbrain tissue of 12-month-old mice. **I**, Quantification of Western blot mitophagy marker expression analysis of ventral midbrain tissue of 12-month-old mice. Results are the mean  $\pm$  SEM,  $n = 8$  per group. Experiments were run in a minimum of experimental triplicate with the average of results used for analysis. ImageJ was used for optical density analysis. Quantifications were normalized to  $\beta$ -actin to account for loading differences and then to wild-type values to normalize against batch effect. Datasets were unbiasedly analyzed using ROUT outlier analysis with a maximum false discovery rate ( $q$ ) of 0.1%. Data were found to be normally distributed via D'Agostino and Pearson test. Data were analyzed using two-way ANOVA ( $F_{(3,28)} = 0.2892$   $p = 0.8328$ ). Uncropped Western blottings for this figure are provided in Extended Data Figure 5-1. **J**, Mitochondrial Complex I activity of ventral midbrain tissue of 12-month-old mice. Results are the mean  $\pm$  SEM,  $n = 6$  per group. Experiments were run in experimental duplicate on one plate with the average of results used for analysis. Datasets were unbiasedly analyzed using ROUT outlier analysis with a maximum false discovery rate ( $q$ ) of 0.1%. Data were found to be normally distributed via Shapiro–Wilk test. Data were analyzed using two-way ANOVA with repeated measures  $F_{(15,18)} = 32.18$   $p < 0.0001$  and a Geisser–Greenhouse's  $\epsilon$  correction of 0.6569. *Post hoc* Tukey's multiple comparisons test was performed and demonstrated no significant (ns) differences between group. The results are as follows:  $p = 0.2569$  for wild-type versus Parkin<sup>-/-</sup>;  $p = 0.9281$  for wild-type versus PolgA<sup>D257A/D257A</sup>,  $p = 0.995$  for wild-type versus Parkin<sup>-/-</sup> versus PolgA<sup>D257A/D257A</sup>, and  $p = 0.9522$  for PolgA<sup>D257A/D257A</sup> versus Parkin<sup>-/-</sup>/PolgA<sup>D257A/D257A</sup>. **K**, Mitochondrial Complex IV activity of ventral midbrain tissue of 12-month-old mice. Results are the mean  $\pm$  SEM,  $n = 6$  per group. Experiments were run in experimental duplicate on one plate with the average of results used for analysis. Datasets were unbiasedly analyzed using ROUT outlier analysis with a maximum false discovery rate ( $q$ ) of 0.1%. Data were found to be normally distributed via Shapiro–Wilk test. Data were analyzed using two-way ANOVA with repeated measures  $F_{(15,18)} = 1.758$   $p = 0.1269$  and a Geisser–Greenhouse's  $\epsilon$  correction of 0.6621. *Post hoc* Tukey's multiple comparisons test was performed and demonstrated no significant (ns) differences between group. The results are as follows:  $p = 0.6015$  for wild-type versus Parkin<sup>-/-</sup>;  $p = 0.2631$  for wild-type versus PolgA<sup>D257A/D257A</sup>,  $p = 0.9822$  for wild-type versus Parkin<sup>-/-</sup> versus PolgA<sup>D257A/D257A</sup>, and  $p = 0.3271$  for PolgA<sup>D257A/D257A</sup> versus Parkin<sup>-/-</sup>/PolgA<sup>D257A/D257A</sup>. Analysis and graphs were produced using GraphPad Prism 9.4.1. The levels of the parkin substrates, NLRP3, AIMP2 normalized to  $\beta$ -actin are presented in Extended Data Figure 5-2.

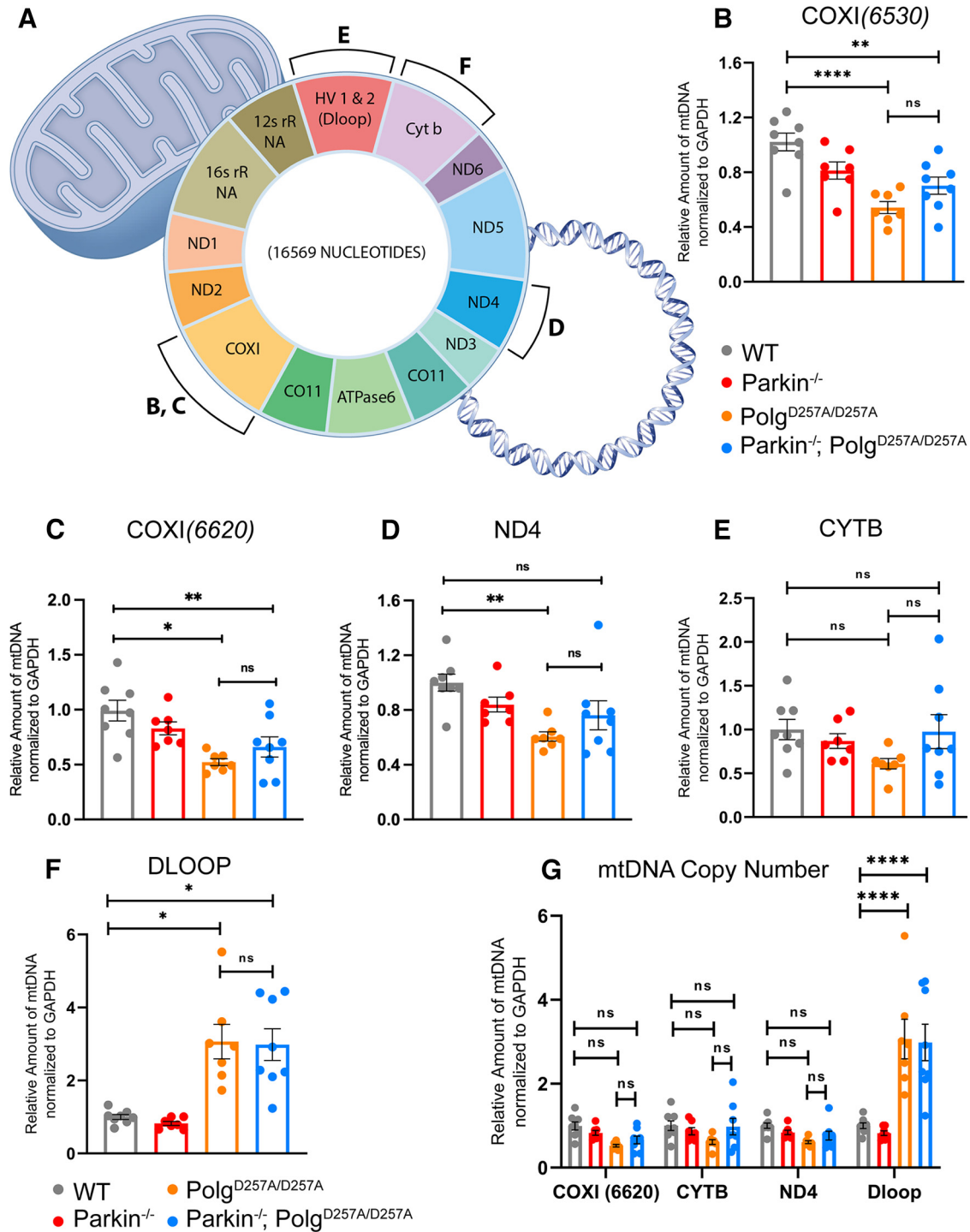


**Figure 6.** Analysis of mtDNA copy number in aged mice. **A**, Schematic denoting mtDNA genome and loci of selected primer sets. Sequences are listed in Materials and Methods. **B–G**, qRT-PCR analysis of ventral midbrain tissue of 12-month-old mice. Results are the mean  $\pm$  SEM,  $n = 6$  mice per group. Experiments run in experimental triplicate with the average of results used for analysis. Quantifications were normalized to GAPDH (COXI6520 to GAPDH\_Neuron, while COXI6620, CYTB, ND4, and Dloop3' were normalized to GAPDH\_PNAS) to normalize variance across groups and then to wild-type values to normalize against batch effect. Datasets were unbiasedly analyzed using ROUT outlier analysis with a maximum false discovery rate ( $q$ ) of 0.1%. SDs did not significantly differ per Brown–Forsythe test. Significance of means analyzed via ordinary one-way ANOVA (**B**:  $F_{(3,26)} = 11.33$  \*\*\*\* $p < 0.00001$ ; **C**:  $F_{(3,26)} = 7.042$  \*\* $p = 0.0013$ ; **D**:  $F_{(3,26)} = 5.130$  \*\* $p = 0.0064$ ; **E**:  $F_{(3,26)} = 1.831$   $p = 0.1663$ ). *Post hoc* Tukey’s test resulted in **B**: \*\*\*\* $p < 0.00001$  for wild-type versus PolgA<sup>D257A/D257A</sup>, \*\* $p = 0.0033$  for wild-type versus Parkin<sup>-/-</sup>/PolgA<sup>D257A/D257A</sup> and \* $p = 0.0236$  for Parkin<sup>-/-</sup> versus PolgA<sup>D257A/D257A</sup>; **C**: \*\* $p = 0.0011$  for wild-type versus PolgA<sup>D257A/D257A</sup>, and \* $p = 0.0205$  for wild-type versus Parkin<sup>-/-</sup>/PolgA<sup>D257A/D257A</sup>; **D**: \*\* $p = 0.037$  for wild-type versus PolgA<sup>D257A/D257A</sup>, ns, not significant. **F**, qRT-PCR analysis of Dloop of ventral midbrain tissue of 12-month-old mice. Results are the mean  $\pm$  SEM,  $n = 6$  mice per group. Experiments run in experimental triplicate with the average of results used for analysis. Quantifications were normalized to GAPDH (GAPDH\_PNAS primer set) to normalize variance across groups and then to wild-type values to normalize against batch effect. Datasets were unbiasedly analyzed using ROUT outlier analysis with a maximum false discovery rate ( $q$ ) of 0.1%. SDs did not significantly differ per Brown–Forsythe test. Significance of means were analyzed via a Welch one-way ANOVA  $W(3.0,13.01) = 14.24$  \*\*\* $p = 0.0002$ . *Post hoc* Dunnett’s T3 multiple comparisons test resulted in \* $p = 0.0237$  for wild-type versus PolgA<sup>D257A/D257A</sup>, \* $p = 0.0142$  for wild-type versus Parkin<sup>-/-</sup>/PolgA<sup>D257A/D257A</sup>, \* $p = 0.0159$  for Parkin<sup>-/-</sup> versus PolgA<sup>D257A/D257A</sup>, and \*\* $p = 0.0088$  for Parkin<sup>-/-</sup> versus Parkin<sup>-/-</sup>/PolgA<sup>D257A/D257A</sup>, ns, not significant. **G**, qRT-PCR analysis of ventral midbrain tissue of 12-month-old mice. Results are the mean  $\pm$  SEM,  $n = 6$  mice per group. Experiments run in experimental

nigral-striatal dependent motor dysfunction in  $\text{Parkin}^{-/-}/\text{PolgA}^{\text{D257A/D257A}}$  mice (Pickrell et al., 2015). We planned to investigate PARIS (Parkin Interacting Substrate, ZNF746) expression and mitochondrial biogenesis dysfunction in this model, with the goal to understand the relative contributions of mitochondrial quality control pathways in PD pathology. Using a variety of behavioral tests, we observed substantial motor and muscular deficits in both  $\text{PolgA}^{\text{D257A/D257A}}$  and  $\text{Parkin}^{-/-}/\text{PolgA}^{\text{D257A/D257A}}$  mice. These deficits were seen at six- and nine-month times with peak dysfunction found at 12 months. Behavioral testing concluded at 12 months as  $\text{PolgA}^{\text{D257A/D257A}}$  mice die prematurely around 13 months of age (Dai et al., 2013; Perier et al., 2013). Locomotor deficits as assessed by openfield were progressive overtime, while deficits in grip strength appeared to fluctuate between timepoints. We speculate these changes in grip strength may be sensitive not only to loss of muscle mass seen in  $\text{PolgA}^{\text{D257A/D257A}}$ -expressing mice, as previously reported (Trifunovic et al., 2004; Kujoth et al., 2005; Hiona et al., 2010; Safdar et al., 2011), but also to changes in body weight, as raw force readings were normalized to total body weight, and both  $\text{PolgA}^{\text{D257A/D257A}}$  and  $\text{Parkin}^{-/-}/\text{PolgA}^{\text{D257A/D257A}}$  cohorts lost muscular mass and body weight overtime. Notably, these deficits were not worsened by the loss of Parkin. Finally, there were no deficits observed via the pole test in 12-month-old mice, demonstrating that behavioral deficits were nonspecific to the nigrostriatal pathway.

The major finding of this paper was that the absence of Parkin in  $\text{PolgA}^{\text{D257A/D257A}}$  mice did not lead to the loss of DA neurons in the SNpc. Immunohistochemical analysis specific to TH+ neurons revealed no loss in the dopaminergic neuronal population of ventral midbrain tissue, and further HPLC assessment found no changes in striatal dopamine. We saw significant reductions in dopamine and serotonin turnover in all  $\text{PolgA}^{\text{D257A/D257A}}$  mice -expressing lines. There was also a decrease in catecholamine concentrations in the olfactory bulb of all mice with the  $\text{PolgA}^{\text{D257A/D257A}}$  mutation; however, loss of Parkin did not lead to further reductions in catecholamine content or turnover. Taken together, these data suggest that there is catecholamine and indolamine dysregulation as a result of the accumulation of mtDNA mutations in  $\text{PolgA}^{\text{D257A/D257A}}$  mice and that loss of Parkin does not enhance this dysregulation.

We also failed to see any substantial changes in expression levels in several mitochondrial markers, including nuclear-encoded subunits of COXI-III. There was, however, a significant reduction in a mitochondrial-encoded subunit of COXIV, likely because of the accumulation of mtDNA indels. Notably, this reduction was not further enhanced by the absence of Parkin. We also failed to see statistically significant changes in Complex I and Complex IV activity between wild-type and  $\text{PolgA}^{\text{D257A/D257A}}$ -expressing mice. This suggests that although there was a reduction in Complex IV expression in  $\text{PolgA}^{\text{D257A/D257A}}$ -expressing mice, the

activity of Complex IV did not decrease. In addition, the  $\text{PolgA}$  mutation did not seem to affect Parkin function, as there was no change in the steady state levels of ubiquitylation substrates of Parkin, including VDAC, AIMP2 and NLRP3 (Y. Lee et al., 2013; Ordureau et al., 2018; Panicker et al., 2022). Furthermore, we observed no changes in expression level of parkin substrates in  $\text{Parkin}^{-/-}$  and  $\text{Parkin}^{-/-}/\text{PolgA}^{\text{D257A/D257A}}$ , further providing evidence for the augmentation of developmental compensatory pathways in  $\text{Parkin}^{-/-}$  mice.

Using a mixed effects model, mtDNA copy number analysis revealed no significant differences in COXI, CYTB, or ND4 copy number between groups. However, there was a significant accumulation of Dloop, the highly conserved origin of replication of mtDNA, in mice with  $\text{PolgA}^{\text{D257A/D257A}}$  knock-in. Individual one-way ANOVA analysis revealed inconsistent results between loci; however, the Dloop copy number remained significantly increased in all  $\text{PolgA}^{\text{D257A/D257A}}$ -expressing mice. This suggests that the conserved Dloop region is significantly less prone to mutations compared with other the other genes tested. As such, the Dloop region amplifies appropriately, while other less conserved regions with mtDNA mutations do not. Alternatively, one could postulate that the  $\text{PolgA}^{\text{D257A/D257A}}$  knock-in may promote the accumulation of advantageous mutations in the Dloop region, which in turn enhances primer annealing and consequential amplification. This may be beneficial to cells as they try to increase replication of mitochondria to combat severe mitochondria dysfunction. This finding is supported by prior work that suggested that accumulation of mitochondrial deletions SNpc dopaminergic neurons in  $\text{PolgA}^{\text{D257A/D257A}}$  mice trigger a compensatory mechanism that include augmenting mtDNA copy number (Perier et al., 2013). Although these data further confirm mitochondrial dysfunction as a result of the accumulation mtDNA mutations because of the  $\text{PolgA}^{\text{D257A}}$  knock-in, they imply that loss of endogenous Parkin in does not synergize mitochondrial dysfunction induced in  $\text{PolgA}^{\text{D257A/D257A}}$  mice.

Studies using germline Parkin knock-out mice have failed to see neurodegeneration, implying that pathways in development likely compensate for its loss and impair the DA neuron degeneration (Fleming et al., 2005). Consistent with this notion are studies that show DA neuronal loss and neurobehavioral deficits when Parkin is conditionally knocked out in adult animals (Shin et al., 2011; Stevens et al., 2015; Y. Lee et al., 2017; Brahmachari et al., 2019; Jo et al., 2021; Panicker et al., 2022; Pirooznia et al., 2022). Because there has been a lack of an obvious Parkinsonian phenotype in germline Parkin null mice, there have been attempts to manipulate other genes in addition to Parkin to promote neurodegeneration. Because of the role of Parkin in mitochondrial quality control, there are a fair number of studies, listed below, in which  $\text{Parkin}^{-/-}$  mice have been crossed to different mouse models of mitochondrial dysfunction. Like our results, the absence of parkin did not enhance the loss of DA neurons and progressive neurodegeneration of the MitoPark mice (Sterky et al., 2011). PD pathology was not worse in PD-mito-Pstl mice, whose mtDNA undergoes double-strand breaks in dopaminergic neurons (Pinto et al., 2018). Crossing parkin KO mice to DJ-1, another autosomal recessive PD gene that affects mitochondrial function (Andres-Mateos et al., 2007) failed to cause a loss of DA neurons. The combined absence of parkin, PINK1 and DJ-1 did not lead to loss of DA neurons (Kitada et al., 2009). Studies in *Drosophila* in which mitochondrial dysfunction and motor deficits driven by an accumulation of mtDNA mutations

←

triplicate with the average of results used for analysis. Quantifications were normalized to GAPDH\_PNAS to normalize variance across groups and then to wild-type values to normalize against batch effect. Datasets were unbiasedly analyzed using ROUT outlier analysis with a maximum false discovery rate (q) of 0.1%. Data were analyzed using the mixed effects model (REML) with matching factors across rows  $F_{(3,80)} = 2.660$ ,  $F_{(3,80)} = 27.20$  \*\*\*\* $p < 0.00001$ ,  $F_{(9,80)} = 10.64$  \*\*\*\* $p < 0.00001$ . Post hoc Tukey's test resulted in \*\*\*\* $p < 0.00001$  for Dloop3' amplification for wild-type versus  $\text{PolgA}^{\text{D257A/D257A}}$ , wild-type versus  $\text{Parkin}^{-/-}/\text{PolgA}^{\text{D257A/D257A}}$ ,  $\text{Parkin}^{-/-}$  versus  $\text{PolgA}^{\text{D257A/D257A}}$ , and  $\text{Parkin}^{-/-}$  versus  $\text{Parkin}^{-/-}/\text{PolgA}^{\text{D257A/D257A}}$ , ns, not significant. Analysis and graphs were produced using GraphPad Prism 8.4.3.

in somatic tissues, failed to show an enhancement of mitochondrial dysfunction or worsening of motor deficits on loss of Parkin (J.J. Lee et al., 2020). A study analyzing the effect of DJ-1 found that DJ-1<sup>-/-</sup>/PolgA<sup>D257A/D257A</sup> mice also failed to synergize with PolgA<sup>D257A</sup> as there was no dopaminergic neurodegeneration or nigral-striatal-dependent motor or enhanced mitochondrial deficits (Hauser et al., 2015).

What might account for the differences between the results presented here and other reports that indicate that mitochondrial dysfunction does not synergize with loss of parkin as reported by (Pickrell et al., 2015)? There are many factors to consider when evaluating biochemical and behavioral differences in Parkin<sup>-/-</sup>/PolgA<sup>D257A/D257A</sup> mice between studies. Animal housing may be a factor, as environment and diet could impact metabolism and gut microbiota, which in turn may affect brain function (Sudo, 2019). In this report we used a Parkin<sup>-/-</sup> line in which the first RING finger domain, encoded by exon 7, is deleted, leading to a catalytically null mutant line (Von Coelln et al., 2004). Because this line was previously reported to display noradrenergic neurodegeneration in the locus coeruleus, we hypothesized the additional mitochondrial dysfunction would surely synergize to induce dopaminergic neuronal loss in the SNpc. Pickrell et al. (2015) used a Parkin<sup>-/-</sup> line in which exon 3 is replaced with EGFP coding sequence, inducing a premature stop codon (Goldberg et al., 2003). This line has no reported dopaminergic neuronal degeneration. Regardless of this difference, we do not believe exon 7 deletion versus exon 3 skipping had a true effect on the study considering the other reports that mice with mitochondrial dysfunction do not synergize with the absence of parkin. Finally, it is important to consider the potential effects of an underpowered study. Our group was sure to sufficiently power our study to avoid a type 2 statistical error.

In conclusion, our results add to the bulk of work which reports germline Parkin knock-out mice do not display neurodegeneration of SNpc dopaminergic neurons. Furthermore, it contributes to findings that report a lack of synergism of Parkin loss on mitochondrial dysfunction in mouse models of mitochondrial deficits. A significant finding in this study is the use of a field accepted method to measure mitochondrial mass. This method relies on the quantification of mtDNA copy number at a DNA level. Here, we show conflicting results of mtDNA quantification. These results appear to be loci dependent, and we hypothesize that the accumulation of mtDNA mutations in PolgA<sup>D257A/D257A</sup> mice directly affect the ability of primers to anneal and amplify appropriately. Consequently, extreme care and consideration should be taken when analyzing mitochondrial mass in *in vivo* models of mtDNA mutations.

## References

- Andres-Mateos E, Perier C, Zhang L, Blanchard-Fillion B, Greco TM, Thomas B, Ko HS, Sasaki M, Ischiropoulos H, Przedborski S, Dawson TM, Dawson VL (2007) DJ-1 gene deletion reveals that DJ-1 is an atypical peroxiredoxin-like peroxidase. *Proc Natl Acad Sci U S A* 104:14807–14812.
- Bonifati V (2014) Genetics of Parkinson's disease—state of the art, 2013. *Parkinsonism Relat Disord* 20 [Suppl 1]:S23–S28.
- Brahmachari S, et al. (2019) Parkin interacting substrate zinc finger protein 746 is a pathological mediator in Parkinson's disease. *Brain* 142:2380–2401.
- Charnay Y, Léger L (2010) Brain serotonergic circuitries. *Dialogues Clin Neurosci* 12:471–487.
- Dai Y, Kiselak T, Clark J, Clore E, Zheng K, Cheng A, Kujoth GC, Prolla TA, Maratos-Flier E, Simon DK (2013) Behavioral and metabolic characterization of heterozygous and homozygous POLG mutator mice. *Mitochondrion* 13:282–291.
- Fleming SM, Fernagut PO, Chesselet MF (2005) Genetic mouse models of parkinsonism: strengths and limitations. *NeuroRx* 2:495–503.
- Ge P, Dawson VL, Dawson TM (2020) PINK1 and Parkin mitochondrial quality control: a source of regional vulnerability in Parkinson's disease. *Mol Neurodegener* 15:20.
- Goldberg MS, Fleming SM, Palacino JJ, Cepeda C, Lam HA, Bhatnagar A, Meloni EG, Wu N, Ackerson LC, Klapstein GJ, Gajendiran M, Roth BL, Chesselet MF, Maidment NT, Levine MS, Shen J (2003) Parkin-deficient mice exhibit nigrostriatal deficits but not loss of dopaminergic neurons. *J Biol Chem* 278:43628–43635.
- Grenier K, McLelland GL, Fon EA (2013) Parkin- and PINK1-dependent mitophagy in neurons: will the real pathway please stand up? *Front Neurol* 4:100.
- Hauser DN, Primiani CT, Langston RG, Kumaran R, Cookson MR (2015) The Polg mutator phenotype does not cause dopaminergic neurodegeneration in DJ-1-deficient mice. *eNeuro* 2:ENEURO.0075-14.2015.
- Hiona A, Sanz A, Kujoth GC, Pamplona R, Seo AY, Hofer T, Someya S, Miyakawa T, Nakayama C, Samhan-Arias AK, Servais S, Barger JL, Portero-Otín M, Tanokura M, Prolla TA, Leeuwenburgh C (2010) Mitochondrial DNA mutations induce mitochondrial dysfunction, apoptosis and sarcopenia in skeletal muscle of mitochondrial DNA mutator mice. *PLoS One* 5:e11468.
- Jo A, et al. (2021) PARIS farnesylation prevents neurodegeneration in models of Parkinson's disease. *Sci Transl Med* 13:eaax8891.
- Kitada T, Asakawa S, Hattori N, Matsumine H, Yamamura Y, Minoshima S, Yokochi M, Mizuno Y, Shimizu N (1998) Mutations in the parkin gene cause autosomal recessive juvenile parkinsonism. *Nature* 392:605–608.
- Kitada T, Tong Y, Gautier CA, Shen J (2009) Absence of nigral degeneration in aged parkin/DJ-1/PINK1 triple knockout mice. *J Neurochem* 111:696–702.
- Kujoth GC, Hiona A, Pugh TD, Someya S, Panzer K, Wohlgemuth SE, Hofer T, Seo AY, Sullivan R, Jobling WA, Morrow JD, Van Remmen H, Sedivy JM, Yamasoba T, Tanokura M, Weindruch R, Leeuwenburgh C, Prolla TA (2005) Mitochondrial DNA mutations, oxidative stress, and apoptosis in mammalian aging. *Science* 309:481–484.
- Lee JJ, Andrezza S, Whitworth AJ (2020) The STING pathway does not contribute to behavioural or mitochondrial phenotypes in *Drosophila* Pink1/parkin or mtDNA mutator models. *Sci Rep* 10:2693.
- Lee Y, Karuppagounder SS, Shin JH, Lee YI, Ko HS, Swing D, Jiang H, Kang SU, Lee BD, Kang HC, Kim D, Tessarollo L, Dawson VL, Dawson TM (2013) Parthanatos mediates AIMP2-activated age-dependent dopaminergic neuronal loss. *Nat Neurosci* 16:1392–1400.
- Lee Y, et al. (2017) PINK1 primes Parkin-mediated ubiquitination of PARIS in dopaminergic neuronal survival. *Cell Rep* 18:918–932.
- Malik AN, Czajka A (2013) Is mitochondrial DNA content a potential biomarker of mitochondrial dysfunction? *Mitochondrion* 13:481–492.
- Mandir AS, Przedborski S, Jackson-Lewis V, Wang ZQ, Simbulan-Rosenthal CM, Smulson ME, Hoffman BE, Guastella DB, Dawson VL, Dawson TM (1999) Poly(ADP-ribose) polymerase activation mediates 1-methyl-4-phenyl-1, 2,3,6-tetrahydropyridine (MPTP)-induced parkinsonism. *Proc Natl Acad Sci U S A* 96:5774–5779.
- Matsuura K, Kabuto H, Makino H, Ogawa N (1997) Pole test is a useful method for evaluating the mouse movement disorder caused by striatal dopamine depletion. *J Neurosci Methods* 73:45–48.
- Ogawa N, Hirose Y, Ohara S, Ono T, Watanabe Y (1985) A simple quantitative bradykinesia test in MPTP-treated mice. *Res Commun Chem Pathol Pharmacol* 50:435–441.
- Ordureau A, Paulo JA, Zhang W, Ahfeldt T, Zhang J, Cohn EF, Hou Z, Heo JM, Rubin LL, Sidhu SS, Gygi SP, Harper JW (2018) Dynamics of PARKIN-dependent mitochondrial ubiquitylation in induced neurons and model systems revealed by digital snapshot proteomics. *Mol Cell* 70:211–227.e8.
- Panicker N, Ge P, Dawson VL, Dawson TM (2021) The cell biology of Parkinson's disease. *J Cell Biol* 220:e202012095.
- Panicker N, Kam TI, Wang H, Neifert S, Chou SC, Kumar M, Brahmachari S, Jhaldiyal A, Hinkle JT, Akkenti F, Mao X, Xu E, Karuppagounder SS, Hsu ET, Kang SU, Pletnikova O, Troncoso J, Dawson VL, Dawson TM (2022) Neuronal NLRP3 is a parkin substrate that drives neurodegeneration in Parkinson's disease. *Neuron* 110:2422–2437.e9.
- Perez FA, Palmiter RD (2005) Parkin-deficient mice are not a robust model of parkinsonism. *Proc Natl Acad Sci U S A* 102:2174–2179.

- Perier C, Bender A, García-Arumí E, Melià MJ, Bové J, Laub C, Klopstock T, Elstner M, Mounsey RB, Teismann P, Prolla T, Andreu AL, Vila M (2013) Accumulation of mitochondrial DNA deletions within dopaminergic neurons triggers neuroprotective mechanisms. *Brain* 136:2369–2378.
- Pickrell AM, Huang CH, Kennedy SR, Ordureau A, Sideris DP, Hoekstra JG, Harper JW, Youle RJ (2015) Endogenous Parkin preserves dopaminergic substantia nigral neurons following mitochondrial DNA mutagenic stress. *Neuron* 87:371–381.
- Pinto M, Nissanka N, Moraes CT (2018) Lack of Parkin anticipates the phenotype and affects mitochondrial morphology and mtDNA levels in a mouse model of Parkinson's disease. *J Neurosci* 38:1042–1053.
- Pirooznia SK, Yuan C, Khan MR, Karuppagounder SS, Wang L, Xiong Y, Kang SU, Lee Y, Dawson VL, Dawson TM (2020) PARIS induced defects in mitochondrial biogenesis drive dopamine neuron loss under conditions of parkin or PINK1 deficiency. *Mol Neurodegener* 15:17.
- Pirooznia SK, Wang H, Panicker N, Kumar M, Neifert S, Dar MA, Lau E, Kang BG, Redding-Ochoa J, Troncoso JC, Dawson VL, Dawson TM (2022) Deubiquitinase CYLD acts as a negative regulator of dopamine neuron survival in Parkinson's disease. *Sci Adv* 8:eabh1824.
- Ross JM, Stewart JB, Hagström E, Brené S, Mourier A, Coppotelli G, Freyer C, Lagouge M, Hoffer BJ, Olson L, Larsson NG (2013) Germline mitochondrial DNA mutations aggravate ageing and can impair brain development. *Nature* 501:412–415.
- Safdar A, Bourgeois JM, Ogborn DI, Little JP, Hettinga BP, Akhtar M, Thompson JE, Melov S, Mocellin NJ, Kujoth GC, Prolla TA, Tarnopolsky MA (2011) Endurance exercise rescues progeroid aging and induces systemic mitochondrial rejuvenation in mtDNA mutator mice. *Proc Natl Acad Sci U S A* 108:4135–4140.
- Shin JH, Ko HS, Kang H, Lee Y, Lee YI, Pletinkova O, Troconso JC, Dawson VL, Dawson TM (2011) PARIS (ZNF746) repression of PGC-1 $\alpha$  contributes to neurodegeneration in Parkinson's disease. *Cell* 144:689–702.
- Sterky FH, Lee S, Wibom R, Olson L, Larsson NG (2011) Impaired mitochondrial transport and Parkin-independent degeneration of respiratory chain-deficient dopamine neurons in vivo. *Proc Natl Acad Sci U S A* 108:12937–12942.
- Stevens DA, Lee Y, Kang HC, Lee BD, Lee YI, Bower A, Jiang H, Kang SU, Andrabi SA, Dawson VL, Shin JH, Dawson TM (2015) Parkin loss leads to PARIS-dependent declines in mitochondrial mass and respiration. *Proc Natl Acad Sci U S A* 112:11696–11701.
- Sudo N (2019) Role of gut microbiota in brain function and stress-related pathology. *Biosci Microbiota Food Health* 38:75–80.
- Tanida I, Ueno T, Kominami E (2008) LC3 and autophagy. *Methods Mol Biol* 445:77–88.
- Trifunovic A, Wredenberg A, Falkenberg M, Spelbrink JN, Rovio AT, Bruder CE, Bohlooly YM, Gidlöf S, Oldfors A, Wibom R, Törnell J, Jacobs HT, Larsson NG (2004) Premature ageing in mice expressing defective mitochondrial DNA polymerase. *Nature* 429:417–423.
- Von Coelln R, Thomas B, Savitt JM, Lim KL, Sasaki M, Hess EJ, Dawson VL, Dawson TM (2004) Loss of locus coeruleus neurons and reduced startle in parkin null mice. *Proc Natl Acad Sci U S A* 101:10744–10749.